In presenting the dissertation as a partial fulfillment of the requirements for an advanced degree from the Georgia Institute of Technology, I agree that the Library of the Institution shall make it available for inspection and circulation in accordance with its regulations governing materials of this type. I agree that permission to copy from, or to publish from, this dissertation may be granted by the professor under whose direction it was written, or, in his absence, by the dean of the Graduate Division when such copying or publication is solely for scholarly purposes and does not involve potential financial gain. It is understood that any copying from, or publication of, this dissertation which involves potential financial gain will not be allowed without written permission.

TURBULENT FLOW IN A THREE-DIMENSIONAL CHANNEL

A THESIS

Presented to

The Faculty of the Graduate Division

by

Hubert Jerome Tracy

In Partial Fulfillment

of the Requirements for the Degree

Doctor of Philosophy in the School of Civil Engineering

Georgia Institute of Technology

October, 1963

TURBULENT FLOW IN A THREE-DIMENSIONAL CHANNEL

Approved:

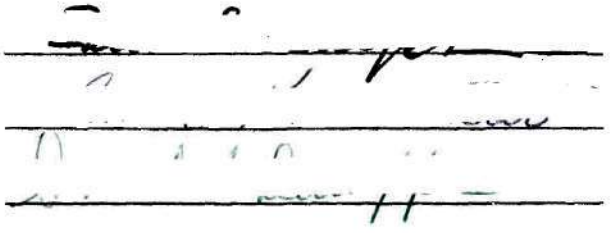

Date approved by Chairman: Aug 13, 1964

ACKNOWLEDGMENTS

The writer is indebted to the School of Aero-Space Engineering of the Georgia Institute of Technology for making available the basic equipment used during this study; to Mr. Edward R. Flynt, Special Research Engineer, Engineering Experiment Station, Georgia Institute of Technology for many hours of patient instruction in hot-wire techniques, and to Mr. Homer J. Bates, Laboratory Technician, for the construction of the experimental conduit and the channel traversing device.

Professor Paul G. Mayer was the thesis advisor; Professors C. E. Kindsvater and A. L. Ducoffe served on the Reading Committee.

The writer wishes to thank the United States Geological Survey for financial support during the research for this thesis.

TABLE OF CONTENTS

TABLE OF CONTENTS (Continued)

LIST OF FIGURES

LIST OF FIGURES (Continued)

LIST OF SYMBOLS

- d - half width of channel (2.5 inches);
- D - channel width (5 inches);
- e - voltage fluctuation;
- P - pressure at any point;
- P^* - piezometric pressure ($P + \gamma y$);
- t - time;
- u - instantaneous value of velocity fluctuation parallel to the direction of mean flow;
- u', v', w' - root-mean-square of velocity fluctuations u, v, w, respectively;
- U - mean velocity in the longitudinal direction at any point in the channel;
- U_o - maximum value of longitudinal mean velocity in the channel (U_o = 40 feet per second);
- U_* - friction velocity $\sqrt{\tau_o/\rho}$;
- U_L - tangential velocity of rotating particle;
- v, w - instantaneous values of velocity fluctuations normal to the direction of the mean flow. The component v is directed upward; the component w is directed laterally;
- V - mean velocity parallel to y-direction at any point in the channel;
- W - mean velocity parallel to z-direction at any point in the channel;
- x - longitudinal coordinate along channel, x = 0 corresponds to channel exit;
- y - vertical coordinate; y = 0 corresponds to channel floor;
- z - lateral coordinate; z = 0 corresponds to channel sidewall;

LIST OF SYMBOLS (Continued)

α,β - angular displacement of sides of elementary particle due to rotation;

γ - specific weight of air;

Γ - circulation in y-z plane;

δ - thickness of laminar sublayer;

θ - angle equal to $\tan^{-1}\frac{w}{U}$;

μ - dynamic viscosity of air;

ν - kinematic viscosity of air;

ξ - rotation in y-z plane;

ρ - air density;

τ_o - shear stress at boundary;

ϕ - angle between axis of hot wire and direction of wind;

ψ - angle between the mean wind and a line parallel to the longitudinal axis of the channel and

∇^2 - Laplacian operator; $\frac{\partial^2}{\partial x^2}+\frac{\partial^2}{\partial y^2}+\frac{\partial^2}{\partial z^2}$.

SUMMARY

The results of velocity measurements in long straight reaches of both open channels and closed conduits have been used in the past as evidence of a pattern of mean motion which consists of a primary component that is essentially longitudinal in direction, with secondary components in the plane of the cross section. The existence of the secondary motion is usually inferred from the configuration of the velocity contours over a normal section.

The cause of the secondary motion has never been satisfactorily explained. It is usually assumed that it is present in any closed conduit of non-circular shape, and in every open channel. It has thus been generally concluded that boundary form is responsible for the motion. Little work has been devoted to the phenomenon since Prandtl, in 1927, explained the occurrence of the circulation by a momentum analysis based upon an assumption that the turbulence fluctuations in the directions tangent to the velocity contours were of greater magnitude than the fluctuations normal to the contours. Prandtl did not give an explanation for the difference in magnitude of the fluctuations. His analysis led to a somewhat different version of the motion than had been given by others. Prandtl's analysis was apparently verified by Nikuradse, who visually observed the distribution of dye injected into the flow.

The purpose of the present study was an examination of the structure of the flow in a non-circular conduit to obtain information relative to the role of the turbulence fluctuations on the secondary motions.

The motion pattern for flow in a corner of a closed conduit or open channel is not subject to complete mathematical analysis, because of the difficulties involved in the solution of the non-linear, partial differential equations of motion. The equations, nevertheless, were used as an analytical basis for the interpretation of the experimental results. Thus, by considering the equations pertinent to the y- and z-directions only, simplifying the problem to a case of uniform motion and neglecting the terms involving purely viscous stress, the equations reduce to:

$$W \frac{\partial \xi}{\partial z} + V \frac{\partial \xi}{\partial y} = \frac{\partial^2 \overline{vw}}{\partial z^2} - \frac{\partial^2 \overline{vw}}{\partial y^2} + \frac{\partial^2}{\partial y \partial z} (\overline{v^2} - \overline{w^2}) \qquad \text{(A)}$$

where:

$$\xi = \frac{\partial W}{\partial y} - \frac{\partial V}{\partial z}$$

and ξ is a measure of the rotation of a fluid particle about the x-axis.

It is shown that a necessary condition for a non-zero value of any of the first four terms of Equation (A) at a point is the existence of V or W; and conversely, that if any of the first four terms exist, then V or W, or both, are not zero. Of primary importance to the existence of the secondary motion, then, is the variation of the normal stress terms $\overline{v^2}$ and $\overline{w^2}$. Little more information can be extracted from Equation (A) without experimental measurement of the quantities involved.

Measurements to define both the mean and the turbulent flow pattern were made in air over a normal section at the downstream end of a rectangular closed conduit 5 inches wide, 32 inches high, and 29 feet

long. A hot wire anenometer was used for the turbulence measurements; mean velocities were measured with a conventional pitot-static tube arrangement. The pressure distribution along the channel was measured, and measurements of the components of the secondary motion, V and W, were obtained with the hot-wire equipment. For the tests the maximum mean velocity in the channel was maintained constant at 40 feet per second, which corresponds to a Reynolds number of about 50,000 based on the half-channel width.

The results of the measurements of the longitudinal mean velocity component over the normal section showed that the flow was symmetrical about the horizontal and vertical centerlines of the channel. The half-section below the horizontal centerline may be divided into two regions; one in the central portion of the channel, and one in the vicinity of the floor. In the central region, the velocities were logarithmically distributed from a point very close to the sidewall outward nearly to the vertical centerline, and the distribution was independent of vertical position. In the floor region, which extended upward to a distance of about ten inches above the floor, the velocities decreased with decreasing distance from the floor; however, the horizontal profiles remained logarithmic for distances above the floor greater than about three inches. At a distance of about three inches above the floor, the horizontal profiles began to flatten at the vertical centerline. Closer to the floor, the point at which the velocity attained its maximum value along each profile was no longer located at the vertical centerline, but was displaced in a direction toward the sidewall.

In the central two-dimensional region, the measurements of the fluctuating components u', v', and w' agreed closely with the distribution

of the corresponding quantities obtained by other investigators in a similar region. A maximum value of each component occurred close to the sidewall, and a minimum value at the vertical centerline. The value at the centerline is very nearly the same for all three components, whereas at the sidewall, u' is greater than the other two, and w' the smallest. The cross-product $\overline{uw}$ had a maximum value close to the sidewall; a zero value at the centerline, and was very nearly linearly distributed between these two points. The quantities $\overline{uv}$ and $\overline{vw}$ were nearly zero throughout this region, as were V and W.

In the floor region, the values of u', v', and w' increased with decreasing distance from the floor. Above a height of about three inches in the channel, however, and except at the vertical centerline, the increase was proportional to the decrease in mean velocity, so that the horizontal profiles of u'/U, v'/U, and w'/U superpose upon the distributions obtained in the central region. Below this height, the velocity fluctuations increase at a faster rate than the decrease in mean velocity. Close to the floor, u' is larger than both v' and w'; however, w' is greater than v'. Distributions of u'/U_o, v'/U_o, and w'/U_o are also shown.

In the floor region (as well as the central region), the variation of the cross-products $\overline{uv}$ and $\overline{uw}$ was shown to depend primarily upon the velocity gradients $\frac{dU}{dy}$ and $\frac{dU}{dz}$, respectively, and in general, the larger the gradients, the larger was the magnitude of these quantities. The variation of $\overline{vw}$, likewise, was dependent upon a gradient in V or W, or both. The maximum values of $\overline{vw}$ were found to be much smaller than those of $\overline{uv}$ and $\overline{uw}$.

The measurements of v' and w' were used in conjunction with Equation (A) to conclude that a secondary motion pattern will be present in any established flow in a non-circular conduit. A physical justification for the measured behavior of v' and w' is obtainable from the consideration that the magnitude of a velocity fluctuation normal to a boundary is inhibited by proximity to the boundary, whereas a similar restriction upon the component parallel to the boundary does not exist.

The measurements of the secondary motion pattern are presented.

CHAPTER I

INTRODUCTION

Description of the Problem

Certain features of the mean velocity distribution over a normal section in long, straight, rectangular open-channels have been the source of speculation in the past. It has often been noted, for example, that the maximum velocity in the vertical was, in some locations, depressed below the water surface. Attention has been called to the fact, also, that the velocities in the vicinity of the corners were somewhat greater than expected. Furthermore, the curves drawn through points of equal velocity (sometimes called isovels) display reversals and curvatures of a singular nature. To a greater or lesser extent, these phenomena are found in open channels of any shape.

The reasons for the occurrence of these events have not been completely explained. It is a well established fact that the irregularities are absent from the velocity distribution in long, straight circular pipes flowing full. On the other hand, the isovel patterns drawn from the results obtained by Nikuradse (1) in a long, rectangular closed conduit exhibit the same general tendencies as those for the open channel, differing only in major aspect near the closed-conduit counterpart of the free surface, which must act as a boundary in the open channel. These circumstances have led investigators to conclude that boundary configuration was responsible for the apparent anomalies in the mean motion pattern.

A physical explanation for the peculiarities in the isovel patterns is obtainable by reference to a system of secondary motions, or superposed circulations, in the plane of the channel cross section. A motion of this kind directed toward the corner regions, for example, will transport particles possessing a relatively higher longitudinal momentum into regions where the particles have a lower momentum. The latter particles will thereby be accelerated until an equilibrium is reached between the momentum so transported and the additional shear stresses created by the higher velocities. For reasons of continuity, the inward flow must be accompanied by an equivalent outward flow along the boundaries, which leads to a system of secondary streamlines which close upon themselves. Similar circulations can usually be deduced in other locations to satisfactorily account for the configuration of any isovel pattern; which is evidence of the existence of secondary motions. The net result of the circulatory pattern is the local transposition of the isovels.

The motivation for the present study was the belief that the generation, mixing, and consequent diffusion of the turbulent eddies from the walls in the vicinity of a corner in a long channel are instrumental to these motions. Its purpose was, therefore, an examination of the structure of the flow in such a region to obtain information relative to the role of the turbulence with respect to the secondary motions.

Scope of the Investigation

The experimental part of the study was carried out in air flow, rather than in water, because instruments for the measurement of turbulence in water have not been perfected. The use of air as a flow medium precluded a free surface; however, neither the use of air nor the absence

of a free surface was believed to place a serious restriction on the extrapolation of the generalized structure of the flow in the vicinity of the conduit corners.

The study was conducted in a rectangular closed channel having an aspect ratio of 1:6.4. The flow was limited to a Reynolds number of approximately 50,000 based on the maximum channel velocity and half-channel width.

The experimental work consisted of the measurement of the mean longitudinal velocity distribution over one section normal to the flow at the downstream end of the channel, the measurement of the distribution of the six components of the Reynolds turbulence stress tensor in the same plane, and the measurement of the transverse mean velocity components in the vicinity of one of the corners of the channel. As well, the variation of the longitudinal pressure gradient was measured.

Review of the Literature

Secondary motions in conduit flow are usually classified according to their origin, and from this standpoint, they belong in one of two general categories. The first of these concern transverse motions which are introduced into the flow as a result of local changes in channel configuration or alignment, or by a local perturbation or disturbance in the flow. Because of the lack of a sustaining mechanism, they decay and disappear downstream from their source. In this category belongs secondary motions resulting from flow around bends, secondary motions caused by the oscillation of solid bodies in fluids (for a discussion of this phenomenon, see Schlichting (2)), and secondary motions which occur in a developing flow in a uniform channel as the mean velocity adjusts to that required by the configuration and roughness of the channel boundaries.

The second kind of secondary motion is the subject of this study, and occurs only in developed flow in prismatic, non-circular channels. The first literature references on this subject were made simultaneously in 1882 by a German, Muller (3), and an American, Stearns (4), apparently independently of one another. In 1909, Gibson (5) published the results of observations concerning the cross motion, without reference to the two preceding papers. Except in minor detail, all three writers were in accord as to the pattern of the motion, and described two symmetrical cells, the movement being directed toward the center of the open conduit at the top, and outward along the bottom. Prandtl (6), in 1927, gave a somewhat different version of the paths followed by the secondary motions. He suggested that they moved along the bisectors of any corner angle toward the corner and then along the adjoining sides away from the corner. Prandtl explained the motion by a momentum analysis based on the assumption that the turbulence fluctuations tangent to the isovels were of greater magnitude than those normal to the isovels. Using this hypothesis, he deduced a momentum distribution having a resultant force pointing toward the convex sides of the isovels (the direction of decreasing velocity); the force having its greatest magnitude where the isovels have the greatest curvature. He credited the production of the secondary motion to this force. He did not explain the difference in magnitude of the fluctuations.

Nikuradse (1), under Prandtl's direction, carried out a painstaking experimental study of flow in conduits having a variety of cross-sectional shapes. Detailed mean velocity measurements were made in each channel. The isovel patterns obtained by Nikuradse in non-circular conduits confirm the general circulation pattern predicted by Prandtl.

Casey (7), for wide shallow channels, suggested a system of multiple circulation cells extending entirely across the channel, with adjacent cells rotating in opposite directions. Vanoni (8) also inferred this pattern from sediment deposits on channel floors. Tracy and Lester (9), however, obtained measurements in smooth rectangular open-channels which permitted the inference that the secondary motions were present only in the regions in the proximity of the two sidewalls of the channel. In this connection, it is to be noted that the existence of a central two-dimensional flow region has been experimentally verified by Bazin (10) in wide, smooth channels, and by Koloseus (11) in artificially roughened channels, among others.

Nemenyi (12) suggested that the secondary motions are of prime importance in their influence on sediment transport. Kirschmer (13) and others have used them to account for channel shape in erodible material, and have attributed high rates of energy loss to their existence. Eckert and Irvine (14) measured the mean velocity field at the end of two triangular ducts for a variety at Reynolds numbers, and, from smoke-visualization techniques, found that both laminar and turbulent flow could exist side by side over a large range of Reynolds numbers. They found no indication of secondary motions except when the flow was strongly turbulent.

Einstein and Li (15) analytically studied the change of vorticity with time in the direction of the main flow, and concluded that secondary motions will not develop spontaneously in laminar motion, but that they could be expected to develop in turbulent flow in regions where the isovels are not parallel. Gessner and Jones (16) made experiments in turbulent flow with no pressure gradient in a rectangular conduit and found that the

isovel pattern at the downstream end of the conduit was essentially independent of the turbulence level of the entering flow, and that the ratio w'/v' was greater than unity in the corner regions of the channel. Delleur and McManus (17) assumed a secondary motion pattern in a rectangular open channel consisting of two cells rotating with a constant angular velocity, and analyzed the motion pattern using the Reynolds equations in cylindrical coordinates to show that the helical motion and the turbulence of the flow were interrelated. Kennedy and Fulton (18) observed discontinuities in curves representing the variation of mean channel velocity at a constant slope as a function of depth from results obtained in a rectangular open channel. They attributed the discontinuities to changes in the pattern of secondary motion with depth; and concluded that the discharge capacity of the channel could be affected by as much as 20 percent by the changes.

Very little material appears in literature more recent than Prandtl's original report (1927) to explain the occurrence of the secondary motions. Most present day hydraulicians have apparently accepted the pattern of motion suggested by Prandtl, and the explanation offered by him.

CHAPTER II

THEORETICAL ANALYSIS OF THE PROBLEM

Equations of Motion

The Navier-Stokes equations are derived from Newton's second law which states that the product of mass and acceleration is equal to the sum of all external forces acting on a body. They are thus momentum equations. At any instant and at any point, they describe both laminar and turbulent flow. For turbulent flow, however, it is usual to modify the equations by substituting for each velocity and pressure term a mean value and the instantaneous deviation therefrom. The time average of the resulting expressions differ from the original statements only by the addition of terms involving the time-averaged velocity fluctuations. The added terms are commonly referred to as "apparent" or "Reynolds" stresses, because they have the dimensions of forces applied to a unit area, and because similar terms were first deduced by Reynolds.

The modified equations, together with the equation of continuity, are a starting point for the description of turbulent flows. The equations, for incompressible flow, and a fluid of constant viscosity in terms of an orthogonal coordinate system, are:

$$\rho \frac{DU}{Dt} = -\frac{\partial P^*}{\partial x} + \mu \nabla^2 U - \rho\left(\frac{\partial \overline{u^2}}{\partial x} + \frac{\partial \overline{uv}}{\partial y} + \frac{\partial \overline{uw}}{\partial z}\right) \qquad (1)$$

$$\rho \frac{DV}{Dt} = -\frac{\partial P^*}{\partial y} + \mu \nabla^2 V - \rho\left(\frac{\partial \overline{uv}}{\partial x} + \frac{\partial \overline{v^2}}{\partial y} + \frac{\partial \overline{vw}}{\partial z}\right) \tag{2}$$

$$\rho \frac{DW}{Dt} = -\frac{\partial P^*}{\partial z} + \mu \nabla^2 W - \rho\left(\frac{\partial \overline{uw}}{\partial x} + \frac{\partial \overline{vw}}{\partial y} + \frac{\partial \overline{w^2}}{\partial z}\right) \tag{3}$$

and the equation of continuity

$$\frac{\partial U}{\partial x} + \frac{\partial V}{\partial y} + \frac{\partial W}{\partial x} = 0 \tag{4}$$

In these equations, the superscript bar is used to denote a time average; D/Dt to refer to the total derivative,

$$\frac{D}{Dt} = \frac{\partial}{\partial t} + U \frac{\partial}{\partial x} + V \frac{\partial}{\partial y} + W \frac{\partial}{\partial z}$$

and ∇^2 to indicate the Laplacian operator

$$\nabla^2 = \frac{\partial^2}{\partial x^2} + \frac{\partial^2}{\partial y^2} + \frac{\partial^2}{\partial z^2}$$

The mathematical difficulties surrounding the integration of the partial-differential, non-linear system of equations listed above are formidable, and solutions have been obtained for only a very few cases. The equations can, nevertheless, be used for experimental guidance, and to furnish an interpretation for the laboratory data.

Two-dimensional Flow

It is appropriate, first, to simplify the equations to apply to the two-dimensional, uniform flow region which is assumed to exist in the

central part of any rectangular conduit of sufficient width and length. The equations, so reduced, are also descriptive of the flow at the inner limits of the three-dimensional regions on either side of the central region. The coordinate axes are orientated as in Figure 1, in order to

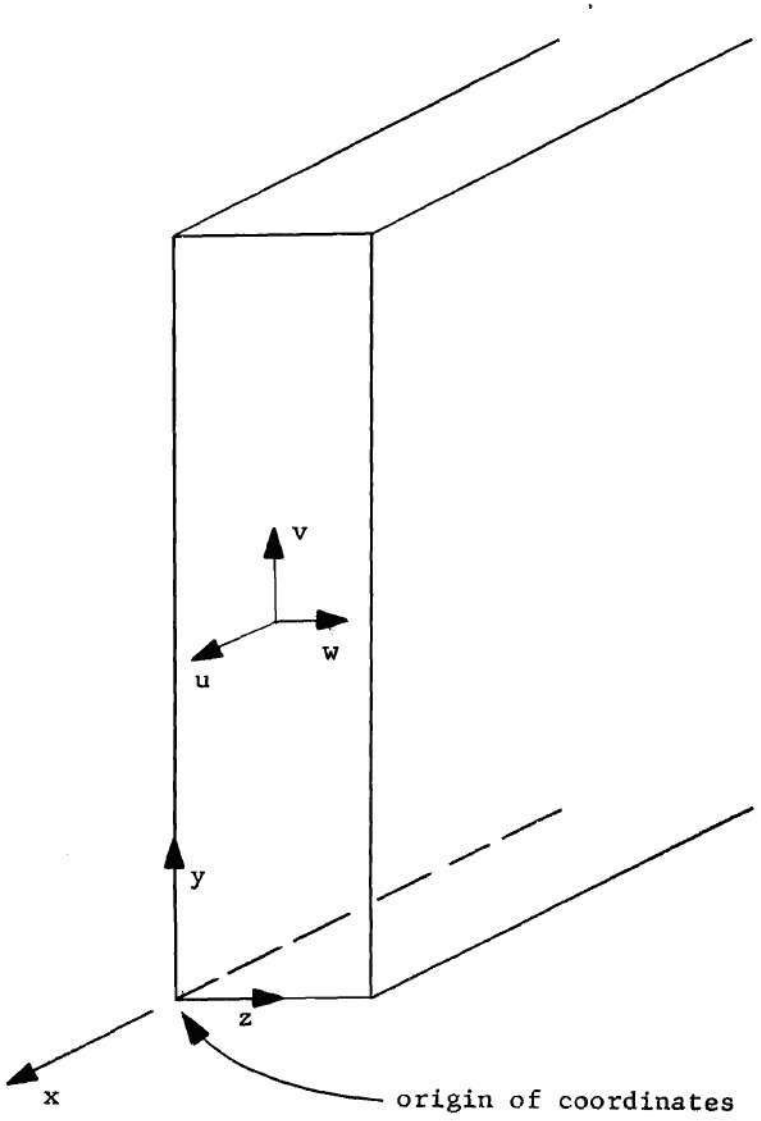

Figure 1. Definition Sketch for Axis Orientation.

conform to the placement of the test channel. The following conditions are assumed to apply:

1. Except for the pressure, all mean quantities are constant in the x-direction,

2. all mean quantities are independent of time,

3. all mean quantities are constant in the direction of the y-axis,

4. $V = 0$. When $V = 0$ and $\frac{\partial U}{\partial x} = 0$, the equation of continuity requires that W be constant; because it is zero at the center line, it must then be zero everywhere in the central region.

Equations (1), (2), and (3) reduce to:

$$0 = -\frac{\partial P^*}{\partial x} + \mu \frac{\partial^2 U}{\partial z^2} - \rho \frac{\partial \overline{uw}}{\partial z} \tag{5}$$

$$0 = -\rho \frac{\partial \overline{vw}}{\partial z} \tag{6}$$

$$0 = -\frac{\partial P^*}{\partial z} - \rho \frac{\partial \overline{w^2}}{\partial z} \tag{7}$$

The second of the equations requires that $\overline{vw}$ be constant. Again, when $\overline{vw}$ is zero at the wall, it must be zero throughout the region.

Equation (7) can be integrated to give

$$P^* + \rho \overline{w^2} = f(x)$$

Because $\overline{w^2}$ is zero at the wall, the pressure is a maximum there.

Differentiating Equation (7) with respect to x:

$$\frac{\partial^2 P^*}{\partial z \partial x} = \frac{\partial}{\partial z}\left(\frac{\partial P^*}{\partial x}\right) = 0$$

which shows that $\frac{\partial P^*}{\partial x}$ is independent of the coordinate z, and Equation (5) can be integrated to yield:

$$\frac{z}{\rho}\frac{\partial P^*}{\partial x} = \frac{\mu}{\rho}\frac{dU}{dz} - \overline{uw} + C$$

The quantity $\frac{dU}{dz}$ is zero at the centerline, from symmetry requirements. The cross-product $\overline{uw}$ is also zero at this point, because $\frac{dU}{dz}$ is zero. This latter can be established by reference to Figure 2. Figure 2 shows

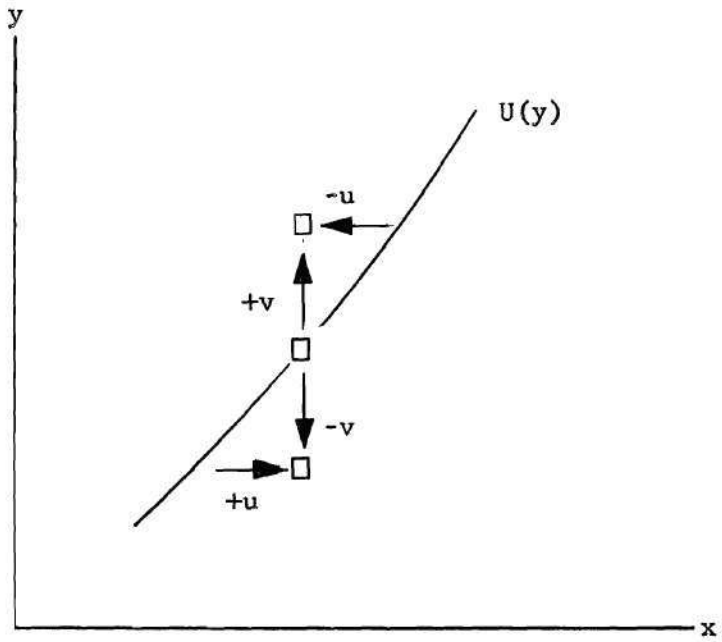

Figure 2. Transport of Momentum Due to Turbulent Velocity Fluctuation.

the coordinate axes Ox and Oz on which is superposed the mean velocity distribution U(z) for which $\frac{dU}{dz}$ is greater than zero. A particle which travels upward as a result of the velocity fluctuation v, moves into a region where, on the average, the mean velocity U is larger than that from the region whence the particle came. If the particle is assumed to maintain its original velocity during its movement, it retards a similar particle at its new position, and thus gives rise to a negative u. Conversely, those particles moving downward, or in a negative direction will be associated with a positive u. Thus, because of the difference in the mean velocity characteristics of the regions corresponding to the original and transposed positions of the particles, the two components of fluctuating velocity will be related, or "correlated," each to the other. As a consequence, their average product will have a value other than zero, and in the case just described, be negative in sign.

On the other hand, if the mean velocity gradient is zero, then upward moving particles migrate into regions having the same mean velocity tendencies as those from which the particles moved. Because the longitudinal turbulence is entirely random, (as is, of course, the vertical turbulence) the transposed particles accelerate or retard particles at their limit of movement in a completely orderless manner; retardation occurring, on the average, just as often as acceleration. This is obviously also true for downward-occurring movement. The vertical migrations, as a result, are not correlated with the longitudinal movement, on the average, and the mean product of u and w is thus equal to zero. It is thus evident that the existence of a mean velocity gradient is a necessary condition in order that the value of the time-mean cross-product of normal components of turbulence be different from zero.

It is thus apparent that a sufficient reason for $\overline{uw} = 0$ at the center of the channel is that $dU/dz = 0$ at that point, and the constant of integration of the last equations is:

$$C = \frac{D}{2\rho} \frac{\partial P^*}{\partial x}$$

and

$$\frac{1}{\rho} \frac{\partial P^*}{\partial x} \left(z - \frac{D}{2} \right) = \frac{\mu}{\rho} \frac{dU}{dz} - \overline{uw} \qquad (8)$$

Thus, the force due to the pressure gradient is expended by direct viscous shear, and by an "apparent" shear due to the correlation of the u and w components of turbulence. The left side of the equation shows that the sum of the two stresses is linearly distributed across the channel, the sum having a maximum value at the wall and a zero value at the centerline. Experimental measurements made in the past have confirmed the fact that, except very close to the wall, almost all of shearing stress is due to the turbulent exchange of momentum. It is to be noted that the shear processes in laminar and turbulent flow are approximately similar. This has led some investigators to represent shear stress in turbulent flow as the sum of two components, thus

$$\tau = (\mu + \eta) \frac{dU}{dz} = \mu \frac{dU}{dz} - \rho \overline{uw}$$

In this equation, the factor η, by analogy with μ, has the significance of a viscosity coefficient and has been called the "eddy" or "apparent" viscosity. It is not, however, a property of the fluid itself, but varies with the magnitude of the turbulence fluctuations.

The conclusions drawn from the preceding discussion are listed below. They state the boundary conditions which are expected to apply at the inner limit of the wall region:

(1) The cross products $\overline{uv}$ and $\overline{vw}$ are zero.

(2) The cross product $\overline{uw}$ is zero at the lateral centerline of the flow, and has a maximum value near the wall. Between these two points, its value varies linearly. The viscous component of shear stress is insignificant except very near the wall.

(3) The piezometric pressure has its maximum value at the wall. Away from the wall, the sum of piezometric pressure and $\rho \overline{w^2}$ is constant.

(4) The mean velocity components in the y and z directions are zero.

Three-dimensional Flow

Not as many terms can be eliminated from Equations (1), (2), and (3) in order that they be applicable to a three-dimensional uniform flow, although some simplification of the equations is possible. First, the assumed condition of steady flow removes the dependency at any quantity on time. Second, the assumed condition of uniform motion causes the mean values of the fluctuating quantities to be independent of the x-direction. Lastly, it will be assumed that the viscous terms of the equations are insignificant (except very close to a fixed boundary), and hence may be neglected. The latter assumption requires only that the Reynolds number be sufficiently high to permit fully developed turbulence to exist.

For these conditions, Equations (1), (2), and (3) reduce to:

$$V \frac{\partial U}{\partial y} + W \frac{\partial U}{\partial z} = - \frac{1}{\rho} \frac{\partial P^*}{\partial x} - \left(\frac{\partial \overline{uv}}{\partial y} + \frac{\partial \overline{uw}}{\partial z} \right) \tag{9}$$

$$V \frac{\partial V}{\partial y} + W \frac{\partial V}{\partial z} = - \frac{1}{\rho} \frac{\partial P^*}{\partial y} - \left(\frac{\partial \overline{v^2}}{\partial y} + \frac{\partial \overline{vw}}{\partial z} \right) \tag{10}$$

$$V \frac{\partial W}{\partial y} + W \frac{\partial W}{\partial z} = - \frac{1}{\rho} \frac{\partial P^*}{\partial z} - \left(\frac{\partial \overline{vw}}{\partial y} + \frac{\partial \overline{w^2}}{\partial z} \right) \tag{11}$$

and the equation of continuity becomes

$$\frac{\partial V}{\partial y} + \frac{\partial W}{\partial z} = 0 \tag{12}$$

Differentiation of Equations (9), (10), and (11) with respect to x, and using the previously stated assumptions, will yield

$$\frac{\partial^2 P^*}{\partial x^2} = \frac{\partial^2 P^*}{\partial y \partial x} = \frac{\partial^2 P^*}{\partial z \partial x} = 0$$

from which it follows that the piezometric gradient at any point of a normal section will not change with distance in the direction of flow. Further, since the order of differentiation may be reversed, it may be concluded also that the gradient with respect to x will not vary from point to point over the section, even though the pressure may not be hydrostatically distributed.

Equation (9) is a statement regarding the momentum balance in the x-direction, and expresses the rate at which the longitudinal pressure force is expended either against the turbulent shear forces or in driving the secondary motion which may be present. While this equation may furnish a link between the longitudinal pressure gradient -- which is the

prime mover for all motion in the channel -- and the secondary motion, it does little to provide an explanation for the origin of the motion.

Because the secondary motions are assumed to be present in corner flows in the plane normal to the longitudinal axis of the channel, a combination and examination of Equations (10) and (11) is indicated. It is convenient, also, to eliminate the pressure terms in the combining process. Thus, differentiating Equation (10) with respect to z, and Equation (11) with respect to y:

$$V\frac{\partial^2 V}{\partial y \partial z} + \frac{\partial V}{\partial z}\frac{\partial V}{\partial y} + W\frac{\partial^2 V}{\partial z^2} + \frac{\partial W}{\partial z}\frac{\partial V}{\partial z} = -\frac{1}{\rho}\frac{\partial^2 P^*}{\partial y \partial z} - \left(\frac{\partial^2 \overline{v^2}}{\partial y \partial z} + \frac{\partial^2 \overline{vw}}{\partial z^2}\right)$$

$$V\frac{\partial^2 W}{\partial y^2} + \frac{\partial W}{\partial y}\frac{\partial V}{\partial y} + W\frac{\partial^2 W}{\partial y \partial z} + \frac{\partial W}{\partial z}\frac{\partial w}{\partial y} = -\frac{1}{\rho}\frac{\partial^2 P^*}{\partial y \partial z} - \left(\frac{\partial^2 \overline{yw}}{\partial y^2} + \frac{\partial^2 \overline{w^2}}{\partial y \partial z}\right)$$

Certain of the terms on the left side of each of the two equations may be eliminated through the use of the continuity equation. Thus:

$$\frac{\partial V}{\partial z}\frac{\partial V}{\partial y} + \frac{\partial W}{\partial z}\frac{\partial V}{\partial z} = \frac{\partial V}{\partial z}\left(\frac{\partial V}{\partial y} + \frac{\partial W}{\partial z}\right) = 0$$

$$\frac{\partial W}{\partial y}\frac{\partial V}{\partial y} + \frac{\partial W}{\partial z}\frac{\partial W}{\partial y} = \frac{\partial W}{\partial y}\left(\frac{\partial V}{\partial y} + \frac{\partial W}{\partial z}\right) = 0$$

the equations reduce to:

$$V\frac{\partial^2 V}{\partial y \partial z} + W\frac{\partial^2 V}{\partial z^2} = -\frac{1}{\rho}\frac{\partial^2 P^*}{\partial y \partial z} - \left(\frac{\partial^2 \overline{v^2}}{\partial y \partial z} + \frac{\partial^2 \overline{vw}}{\partial z^2}\right)$$

$$V\frac{\partial^2 W}{\partial y^2} + W\frac{\partial^2 W}{\partial y \partial z} = -\frac{1}{\rho}\frac{\partial^2 P^*}{\partial y \partial z} - \left(\frac{\partial^2 \overline{vw}}{\partial y^2} + \frac{\partial^2 \overline{w^2}}{\partial y \partial z}\right)$$

Subtracting the lower equation from the upper:

$$W\left(\frac{\partial^2 V}{\partial z^2} - \frac{\partial^2 W}{\partial y \partial z}\right) + V\left(\frac{\partial^2 V}{\partial y \partial z} - \frac{\partial^2 W}{\partial y^2}\right) = \frac{\partial^2 \overline{vw}}{\partial y^2} + \frac{\partial^2 \overline{w^2}}{\partial y \partial z} - \frac{\partial^2 \overline{v^2}}{\partial y \partial z} - \frac{\partial^2 \overline{vw}}{\partial z^2}$$

or,

$$W\left[\frac{\partial}{\partial z}\left(\frac{\partial V}{\partial z} - \frac{\partial W}{\partial y}\right)\right] + V\left[\frac{\partial}{\partial y}\left(\frac{\partial V}{\partial z} - \frac{\partial W}{\partial y}\right)\right] = \frac{\partial^2 \overline{vw}}{\partial y^2} - \frac{\partial^2 \overline{vw}}{\partial z^2} + \frac{\partial^2}{\partial y \partial z}\left(\overline{w^2} - \overline{v^2}\right)$$

which can be written:

$$W\frac{\partial \xi}{\partial z} + V\frac{\partial \xi}{\partial y} = \frac{\partial^2 \overline{vw}}{\partial z^2} - \frac{\partial^2 \overline{vw}}{\partial y^2} + \frac{\partial^2}{\partial y \partial z}\left(\overline{v^2} - \overline{w^2}\right) \qquad (13)$$

where

$$\xi = \frac{\partial W}{\partial y} - \frac{\partial V}{\partial z}$$

The quantity ξ is a measure of the rotation of a fluid particle about an axis normal to the y-z plane. This may be shown by reference to Figure 3 on which is drawn one face of a cubical element orientated so as to lie in the y-z plane, and which undergoes rotation in that plane. The rotated position of the face is indicated by the dashed lines. The total angle through which the face is rotated is equal to the average of the two angles $d\alpha$ and $d\beta$, whose values may be considered numerically equal to their respective tangents, since they are small. If the counterclockwise direction is positive, the total angle is

$$\frac{d\alpha + d\beta}{2} = \frac{1}{2}\left(\frac{\partial V}{dz} - \frac{\partial W}{dy}\right) dt$$

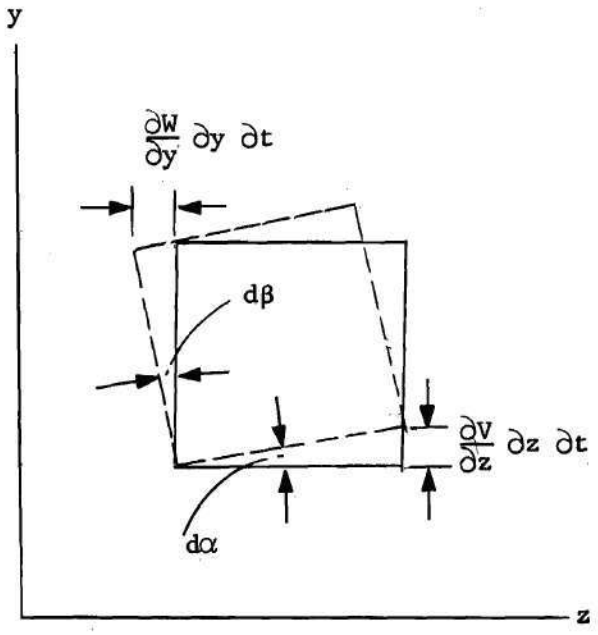

Figure 3. Schematic Representation of Rotation

and the rate of rotation

$$\frac{1}{2}\left(\frac{\partial V}{dz} - \frac{\partial W}{dy}\right)$$

Mathematically, the rotation phenomenon is closely allied to the concept of circulation which is usually denoted by the symbol Γ, which is defined as the line integral of tangential velocity about any closed curve

$$\Gamma = \oint_L U_L \, dL \tag{14}$$

The path followed by the curve may be completely arbitrary. If such a surface is divided into a number of similiarily arbitrarily shaped

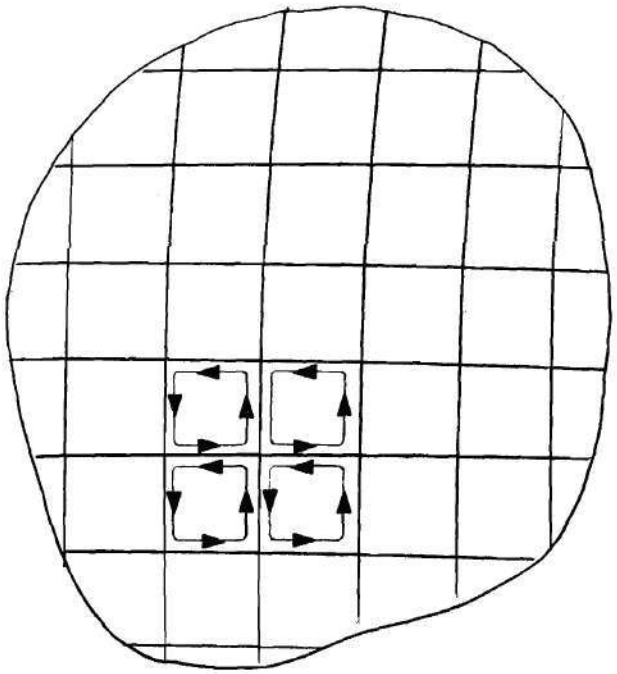

Figure 4. Schematic Representation of Circulation

subregions, reference to Figure 4 will show that the circulation around the larger enclosing curve is equal to the sum of the circulations around the smaller regions, because the line integrals around the boundaries of the latter will be of opposite sign to those of the adjacent boundaries of the neighboring elements. Only when the boundaries are coincident with those of the enveloping curve will a resultant exist, the sum of which is simply the circulation around the outer curve. Moreover, it is not difficult to show, as the area of any surface becomes very small, that the circulation around the surface, per unit of area, is equal to

twice the rotation, or

$$\lim_{A \to 0} \frac{\Gamma}{A} = 2\xi \qquad (15)$$

The evaluation of the incremental circulations in accordance with Equation (15), and their summation around any closed curve in the plane normal to the x-axis is the circulation around the surface so chosen. If the selected path is coincident with one of the streamlines of secondary motion, the result is a measure of the strength of motion.

The concept of rotation -- and its mathematical definition -- allow a physical interpretation of the first two terms of Equation (13). The angular velocity ξ is a vector whose direction is normal to the plane of rotation. The terms involving ξ are the substantial derivative of this velocity (with the t- and x-dependent terms equal to zero), and thus describe the rate of change of the rotation of a particle in the y-z plane. By inspection, it is obvious that both terms vanish if V and W, which are the components of the secondary motion, are zero. On the other hand, the existence of either term, or an algebraic resultant, requires that V or W, *or both, be not equal to zero.*

The latter statement is equally applicable to the first two terms on the right side of the equation, which contain the average product of v and w. The correlation of v and w, with the result that the average value of their product is other than zero, requires a gradient in the mean velocity counterpart of at least one of the two fluctuating elements. Thus, the least that is required in order that the terms involving $\overline{vw}$ in combination not be equal to zero is the existence of a secondary motion, whatever else is implied by the second order differentials.

Thus, a non-zero value of any of the first four terms of Equation (13), or their resultant sum, implies a secondary motion at the point under consideration. The resultant will obviously exist if the last term of the equation is not zero, in order that the equation be balanced.

The first four terms of the equation are descriptive of secondary motion, or of its effect, rather than of its cause. On the other hand, the variation of the last term, which involves v and w, is not directly related to the motion, but instead is dependent upon the configuration of the boundaries of the channel. Thus, in a later part of this report, the variation of this term will be examined in the light of the conclusions of the preceding discussion.

CHAPTER III

EXPERIMENTAL EQUIPMENT AND TECHNIQUES

Wind Tunnel

The experimental measurements were made in a closed conduit installed in a low-turbulence wind tunnel located in the School of Aerospace Engineering of the Georgia Institute of Technology. The tunnel has been completely described by Ducoffe (19). A sketch of the tunnel is shown on Figure 5. It was operated by a direct-current motor which drives a four-bladed fan. The speed was controlled by varying the current to the drive motor. The turbulence level prior to the working section was reduced effectively by an 8-inch honeycomb and a series of fine-mesh, seamless bronze screens followed by a 10:1 contraction.

The working section of the original tunnel was square, 42 inches on each side, and had a length of 20 feet. Both vertical walls were removed from the facility during the installation of the experimental channel. The experimental channel was 5 inches wide and 32 inches high. It consisted of four smoothly joined sections, three having lengths of 8 feet, and one a length of 5 feet. The total length of the channel was thus 29 feet. The installation is shown schematically on Figure 5.

One of the 8-foot sections was made of 3/4-inch interior grade plywood, and was installed at the upstream end of the channel. The downstream sections were constructed from 1/2-inch plexiglas sheets, which were supported on a system of 3/8-inch threaded steel rods tapped into small 1/2-inch-thick plastic inserts cemented to the outside of the

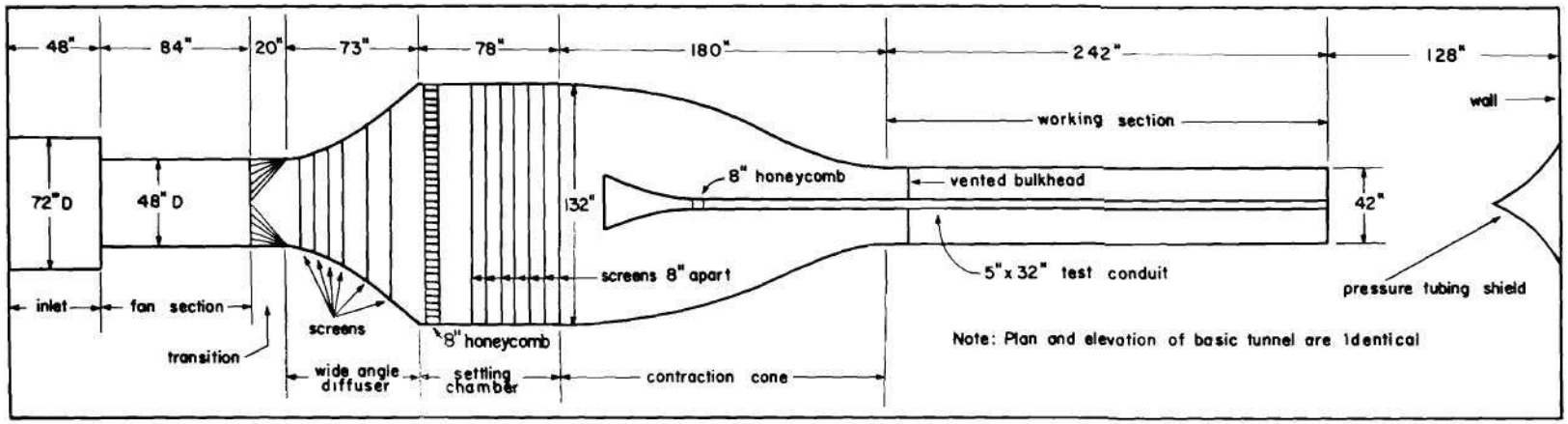

Figure 5. Schematic of Low Turbulence Wind Tunnel and Test Conduit.

vertical walls and to the lower side of the bottom segment. The threaded rods projected through holes drilled into the sides and bottom of a series of rectangular frames made of 2 x 2-inch aluminum angle and placed on approximate 3-foot centers along the length of the channel. Bolts on the threaded rod, one on each side of the flat side (with respect to the channel) of the frame angles permitted the walls and floor of the channel to be brought into plane alignment by adjustments in the length of the rod projecting from the supports. Five rods were used on each vertical side of each frame; one located three inches below the top and one three inches above the bottom of the channel, with the remaining three spaced between these two on approximate 9-inch centers. Two rods were used on the bottom piece, and were spaced on the third points. The upper part of the channel was bolted to the supporting frames.

The upper end of the channel extended into the expanded section, or settling chamber, of the larger tunnel, both to provide greater length for flow development and to place its intake in a region where the velocities were relatively low. A bell-shaped entrance, flared on all four sides, four feet in length, was placed at the upstream end of the channel. A honeycomb, consisting of thin-walled, 1-inch steel pipe eight inches long was inserted just downstream from the flared entrance, at the beginning of the 5-inch plywood channel. End and side views of the installation are shown on Figures 6a and 6b.

Piezometer outlets 1/32 inch in diameter were drilled into the floor along its centerline at 1-foot intervals for the last 20 feet of the channel.

Initially, an air-tight bulkhead was placed between the outside walls of the channel and the inside walls of the basic tunnel, and was

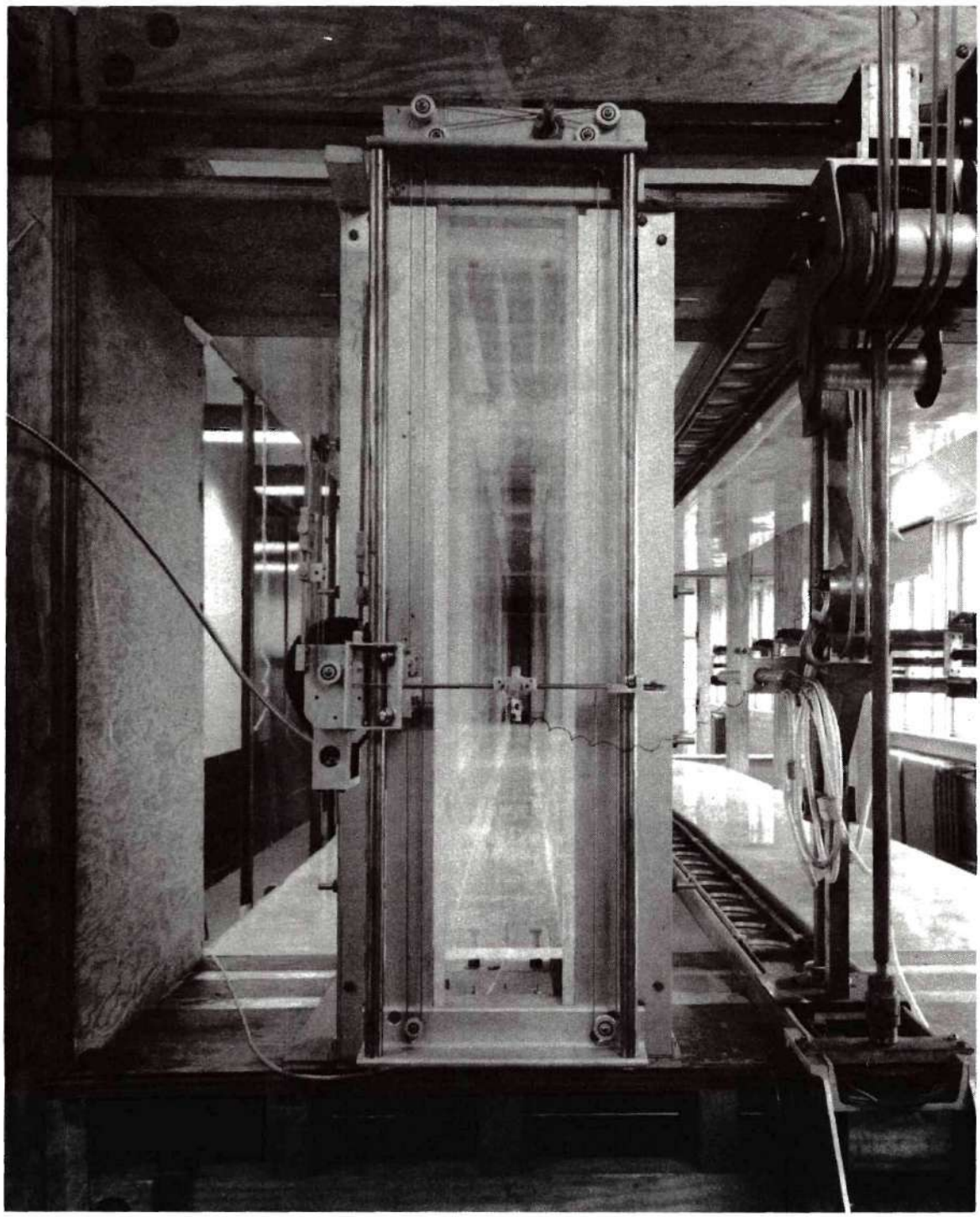

Figure 6a. End View of Channel.

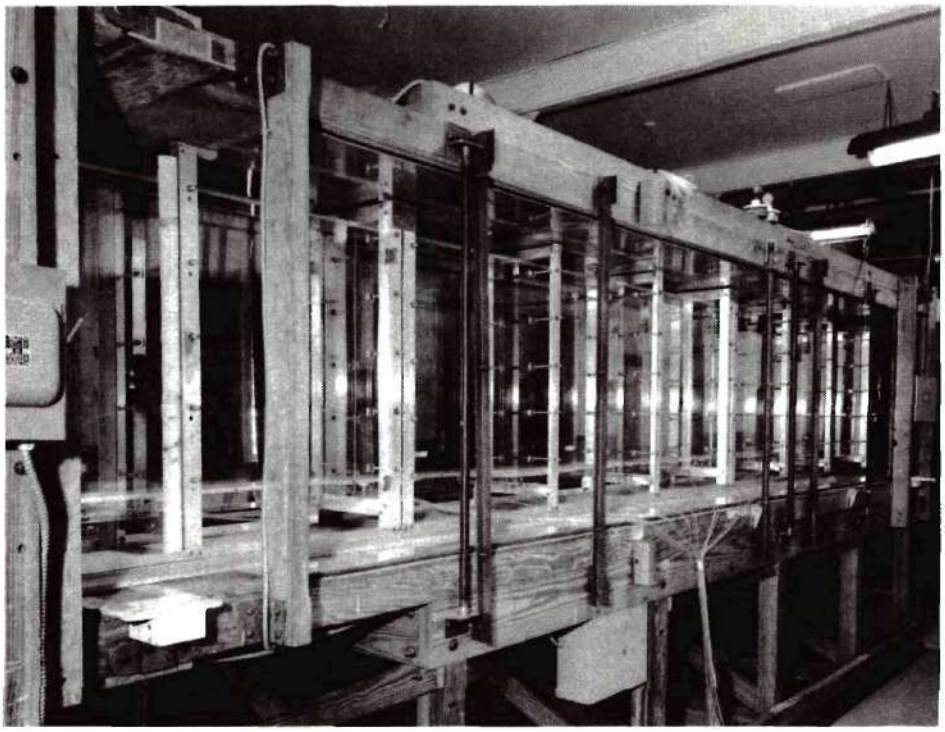

Figure 6b. Side View of Channel.

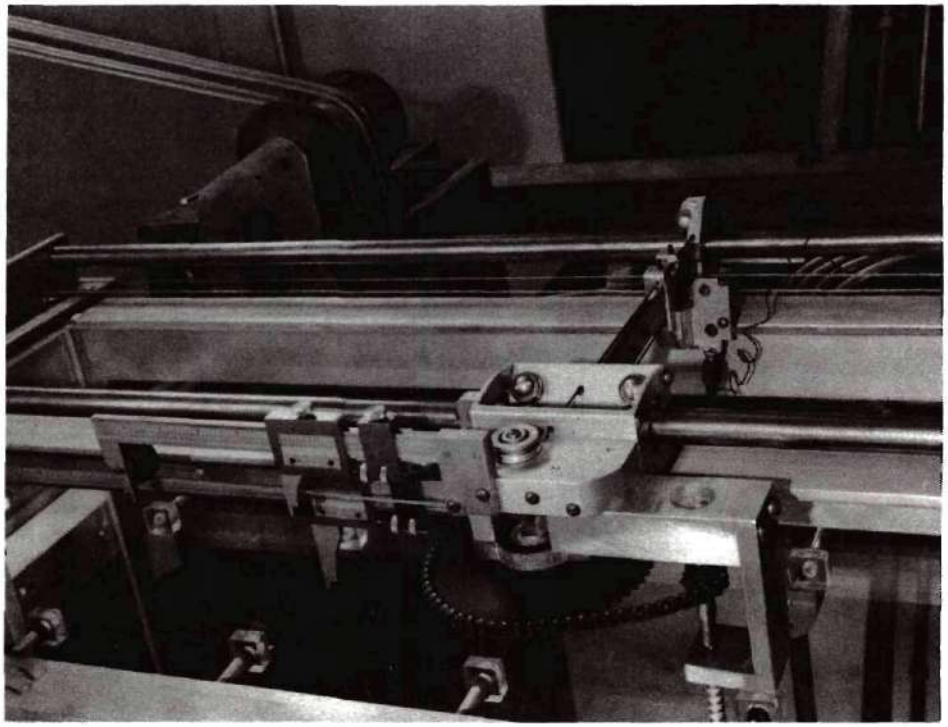

Figure 6c. Traversing Scale Indicators.

located seven feet downstream from the end of the entrance cone. During the preliminary tests, however, the bulkhead was vented to reduce surges in the system.

Traversing Mechanism

All measurements were made over a normal section six inches upstream from the channel exit. An exception was measurements to ascertain the state of development of the flow.

The probe holder consisted of a segmented steel block, constructed to fit snugly around, and to slide along, a section of flat tool-steel bar which served as the horizontal traversing support. The flat bar was 8-1/2 inches long, 1/8 inch thick, and 3/4 inch wide. The sliding block was restrained against pitch and yaw by lengths of pre-tensioned spring steel inserted between holder and bar at the top and front of the bar.

Vertical movement of the probe was guided by lengths of 3/4-inch machined steel bar, attached vertically at each side of the channel to a rectangular frame built of aluminum angle. The frame was bolted to the channel sides. The vertical steel bars served as guide rails for brackets attached to each end of the traversing bar. The brackets were held against the rails by a number of press-fitted ball-bearing rollers, so arranged in combination to restrain all movement of the traversing bar except the desired vertical motion. A continuous length of 1/16-inch stranded-steel cable, attached to each bracket and thence over and around a series of six pulleys at the top and bottom of the mounting frame insured like vertical movement of each bracket, and operated in much the same manner as the cable and pulley arrangement used on parallel rulers found on

drawing boards. When mounted, the traversing bar moved in a plane approximately one-half inch downstream from the exit of the channel.

The position of the various probes with respect to the channel sidewall was indicated on a graduated 6-inch scale attached in a vertical position to one of the brackets. A continuous length of 1/16-inch stranded-steel cable attached to the clamping-lock side of the scale and to the sliding block on the traversing bar through a series of pulleys enabled the relative motion of the block to be transferred to the scale. A simultaneous determination of the probe position relative to the sidewall and a movement of the vernier slide relative to the clamping slide on the scale to indicate the measured probe position served to orientate the probe for horizontal movement. The details of the mechanism may be seen in Figures 6b and 6c.

The vertical position of the probe was referenced to the channel floor, and was measured on a 12-inch scale affixed in a vertical position side by side with the 6-inch scale on the same bracket. The clamping lock slide of the scale was bolted to the frame of the traversing device. Vertical orientation of the probe was obtained by a procedure similar to that described for the horizontal. Traverses at distances greater than 12 inches above the channel floor were made by re-attaching the clamping-lock slide of the scale to the frame at suitable alternate locations. Both the 6-inch and the 12-inch scale could be read to the nearest 0.001 inch.

The hot-wires were positioned relative to the floor and to the sidewall by placing the wires an arbitrary distance close to the wall (or floor) somewhat less than 0.050 inch. The distance between the wire and its image in the glass were then measured by use of a forty-power

microscope having a scale readable to 0.0002 inch imprinted on its focal plane. Half of the observed distance between wire and image was then set on the appropriate graduated scale.

In use, the reverse ends of the probe stems were inserted into a socket device attached to the underside of the sliding block on the traversing rod. The socket mount could be turned to either side, or up or down, through angles up to about 20 degrees. In addition, the probe stem could be rotated in the socket itself.

The apparatus and procedure described above enabled the probes to be positioned in the measuring plane to an accuracy perhaps between 0.001 and 0.002 inch in each of the two coordinate directions.

Hot-Wire Equipment

Turbulent measurements were made using constant-current, Thiele-Wright hot-wire anemometer equipment. The frequency response of the amplifier was essentially flat up to about 25,000 cycles per sound. In order to minimize the amplifier noise level, however, a filter to limit the signal frequency passed through the amplifier to 5,000 cps was inserted in the circuit. Although a very small portion of the turbulent energy present in the channel was known to be in a frequency range equal to or greater than 5000 cps, no detectable difference in signal could be observed when comparative measurements were made with the filter removed.

The wires were compensated for thermal lag by the square-wave method. Output readings were taken with a thermocouple and precision microammeter. The amplifier, thermocouple, and microammeter were calibrated against a known RMS sine-wave signal.

The hot wire probes were constructed by soft-soldering 0.0001-inch diameter platinum-rhodium (90 per cent platinum and 10 per cent rhodium) wire drawn by the Wollaston process to the tips of fine sewing needles (Sharps No. 11) after the silver coating had been etched off the wire in a dilute nitric-acid solution. A single-wire probe was used to measure u'; cross- or x-wires to measure shearing stress and the lateral and vertical components of turbulence.

The tips of the needles were spaced 0.030 inch apart for the u' probe. For the cross-wire meters, the tips of the pairs of needles had a lateral spacing of 0.040 inch. The wires for the v' and w' meter subtended a central angle of 60 degrees, those for the $\overline{uv}$ and $\overline{uw}$ measurements a central angle of 90 degrees. The wire lengths for the v' and w' probes were thus 0.069 inch and for the $\overline{uv}$ and $\overline{uw}$ probe, 0.056 inch. A 60-degree cross-wire probe was used in the measurement of $\overline{vw}$. The pairs of wires were spaced 0.025 inch apart for all cross-wire probes.

Six-inch lengths of 3/8-inch brass tubing were used as supports for the needles to place their tips upstream in the tunnel sufficiently far to be free from adverse affects due to the proximity of the end of the channel. The needles extended from the end of the tubes a distance of about two inches. The conducting leads were carried back through the tubes to connections at the side of the tunnel. The tubes themselves could be bent to any desired curvature to facilitate placing the wires with respect to the channel walls. The reverse ends of the tubes were inserted into the socket fitting described earlier.

With the exception of those related to the determination of the shear component $\overline{vw}$, the techniques involved in the measurement of the

three components of turbulence and the other two shear terms are well known, and have been detailed in the literature. One such source for this material is reference (20), and the methods outlined in that report have essentially been followed during the present study. To supplement that instruction, however, two methods suitable for the measurement of $\overline{vw}$ will be described briefly.

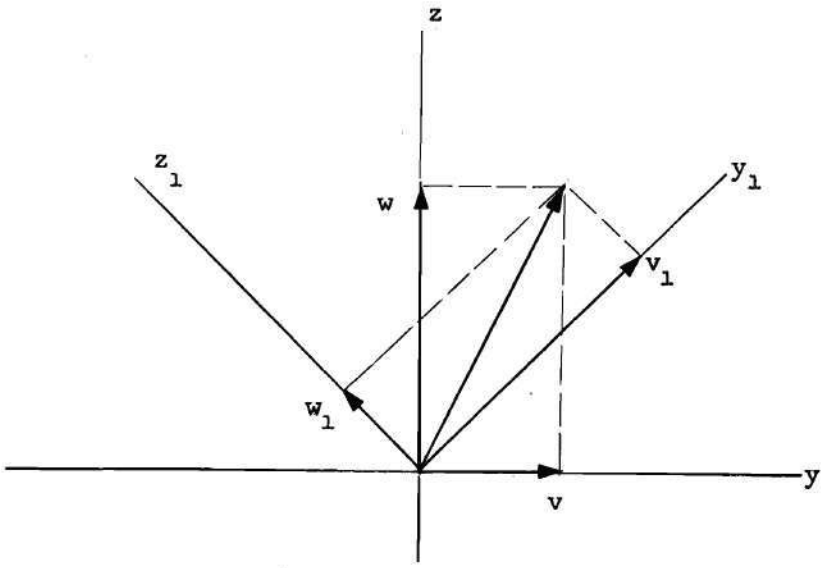

Figure 7. Axis Orientation for Measurement of $\overline{vw}$.

For the first, reference is made to Figure 7 on which two axes Oy_1 and Oz_1 are located on the bisectors of the orthogonal axes Oy and Oz. If the components of turbulence parallel to the Oy, Oz, Oy_1 and Oz_1 are denoted, respectively, by v, w, v_1, and w_1, the following relationships are obtained by the resolution of v and w into components parallel and normal to the Oy_1 and Oz_1 axes:

$$v_1 = \frac{1}{\sqrt{2}} (v + w)$$

$$w_1 = \frac{1}{\sqrt{2}} (- v + w)$$

Squaring, and taking time averages:

$$\overline{v_1^2} = \frac{1}{2} (\overline{v^2} + \overline{w^2} + 2\ \overline{vw})$$

$$\overline{w_1^2} = \frac{1}{2} (\overline{v^2} + \overline{w^2} - 2\ \overline{vw})$$

Subtracting:

$$\overline{vw} = \frac{1}{2} (\overline{v_1^2} - \overline{w_1^2})$$

The fluctuating quantities $\overline{v_1^2}$ and $\overline{w_1^2}$ are measured with 60 degree cross-wires orientated on the Oy_1 and Ox_1 axes. The method used is exactly the same as for the $\overline{v^2}$ and $\overline{w^2}$ components.

Hinze (21) outlines an alternate method for the measurement of $\overline{vw}$ which utilizes two identical slanting wires, each subtending the same angle to the mean flow direction. By placing wire 1 in the x-y plane and wire 2 in the x-z plane at the same point in space, the instantaneous signals given by each wire are:

$$e_1 = Au + Bv$$

$$e_2 = Au + Bw$$

where A and B are constants defined in the Schubauer-Klebanoff (20) report and are determined by direct calibration. By subtracting the instantaneous signals, squaring, and averaging; one obtains:

$$\overline{(e_1 - e_2)^2} = \overline{(Au + Bv - Au - Bw)^2}$$

from whence:

$$- \overline{vw} = \frac{\overline{(e_1 - e_2)^2}}{2\,B^2} - \frac{(\overline{v^2} + \overline{w^2})}{2}$$

the use of this result depends upon a prior knowledge or independent measurement of $\overline{v^2}$ and $\overline{w^2}$.

A second series of measurements may be used to eliminate $\overline{v^2}$ and $\overline{w^2}$ from the last equation. If wire 2 is rotated through 180 degrees, one obtains

$$- \overline{vw} = - \frac{\overline{(e_1 - e_2)^2}}{2\,B^2} + \frac{(\overline{v^2} + \overline{w^2})}{2}$$

Designating the squared difference in signal before and after rotation by the subscripts a and b, respectively, the two expressions for $\overline{vw}$ may be added to yield:

$$- 2\,\overline{vw} = \frac{\overline{(e_1 - e_2)_a^2} - \overline{(e_1 - e_2)_b^2}}{2\,B^2}$$

Neither of the two methods appear to offer an apparent advantage over the other from an experimental standpoint. Both are tedious and not

characterized by results of a high degree of accuracy. The first of the two procedures was arbitrarily selected for use during this study. No other procedures for this measurement are known.

The hot wires were calibrated in place in the tunnel. For the probes requiring a calibration only against mean velocity (those for the measurement of u', $\overline{uv}$, and $\overline{uw}$), a rating curve for mean velocity at a selected point in the measuring section (this point was at the center of the channel, 10 inches above the floor) against pressure differences between the settling chamber and the most downstream piezometer was constructed, using a pitot-static tube for the velocity determinations. The variation in velocity was obtained by varying the fan speed. For calibration, the probes were placed at the selected point, and the pressure-velocity rating curve used to establish the necessary fan speed to obtain the desired mean velocity.

For those probes calibrated by measurements of voltage differences between wire pairs as a function of stem angle and velocity (those for the measurement of v', w', and $\overline{vw}$), the procedure just described sufficed to establish the necessary known point velocity. Variations in stem angle were measured through the use of a 6-inch protractor attached to the back of the probe mounting slide in conjunction with a needle indicator. Angles could be measured within about one-quarter of one degree.

In the corner regions, secondary motions caused the mean direction of flow to be other than parallel to the longitudinal axis of the channel. Because both wires of a pair of cross-wires must subtend the same angle with respect to the mean wind for correct measurement, it was necessary to compensate for the variation in flow direction by a corresponding

realignment of the probe in traversing from point to point in the flow. This feature added considerably to the level of difficulty of measurements involving two-wire probes. At the same time, however, the sensitivity of this type of meter to direction made possible the direct measurement of the horizontal and vertical components of the secondary motion.

The procedure used to sense changes in the direction of flow consisted of the determination of the steady-state voltage across each wire of a pair separately at each measurement point. A voltage balance, on the one hand, signalled a corresponding resistance balance (for constant-current operation with matched wires) which, in turn, indicated that both wires were cooled alike by the mean flow, and that they thus subtended the same angle to the mean direction of flow. A difference in voltage, on the other hand, was an indication of unlike subtended angles; which was then rectified by an adjustment in the orientation of the probe stem. After the necessary adjustment to obtain equal voltage readings for both wires, the appropriate turbulence signals were read.

The voltage unbalance is also a measure of the angle between the velocity vector parallel to the probe and the vector normal to it in the plane of orientation. Thus, a traverse with the probe always parallel to the longitudinal axis of the channel will yield voltage signals at each point which are proportional to the angle between the U component of velocity and the V or W component, depending upon the plane in which the wires are placed. The voltage readings may be converted into angular measures by a calibration procedure in which voltage difference is measured as the stem angle is systematically varied in the plane of orientation in a known mean velocity field.

For the measurement of the components of the secondary motion, a calibrated cross-wire probe was first placed in the central region of flow at the horizontal centerline of the channel -- that is, at a point where both V and W are zero. For the determination of V, the wires were in the x-y plane; and for W, in the x-z plane. In each case, at this point, the instrument was orientated so that it was parallel to the mean wind -- i.e., so that the voltage in both wires were the same. The flow field was then traversed without a further change in probe alignment.

The measured quantities v' and w' are the root-mean squares of the velocity fluctuations normal to the direction of the mean flow. They are not, because of the variations in mean flow direction due to the secondary motion, always directed vertically and horizontally. The correction to the measured values to account for the change in direction is $(1 - \cos \psi)$, where ψ is the angular deviation of the mean flow from a line parallel to the longitudinal axis of the channel. Because ψ has a maximum value of about two degrees the error from this source is less than one-tenth of one per cent. No correction has been applied to the measured turbulence quantities.

Through continued practice and the exercise of patience, the slanting wires on the various probes could always be matched so that the cold resistance of a given pair differed by less than one per cent. No difficulty with wire breakage under operating conditions was experienced; however, a great number of wires were broken in installing the probes in the tunnel. Almost any slight jar or bump was usually sufficient to part the wires, because they were always under some tension.

Errors in Hot-Wire Measurements

The errors in hot-wire anemometry -- as well as in any other measurement -- can be listed in one of two general classes. The first includes those errors classified as "experimental." To be listed here are shortcomings in equipment and experimental techniques, which, to some degree, involves each piece of physical equipment and procedure in the whole.

An indication of the net effect of this type of error is usually given by the precision with which a given set of measurements can be repeated, and this is perhaps more reliable than an attempt to assess and to combine individual errors. Remeasurement of sets of data during the course of the experimental work indicate a repeatable limit for the various fluctuating quantities to be about 2 per cent for u', 4 per cent for v' and w', 8 per cent for $\overline{uv}$ and $\overline{uw}$, and a much greater value for $\overline{vw}$.

The second class of errors is connected to the practical impossibility of constructing a device to conform exactly with the theoretical model. In hot-wire anemometry, the effects of the factors listed below contribute to errors that fall into this general classification. These are:

1. Neglect of one velocity component,
2. large turbulent fluctuations,
3. nonuniform velocity distribution along a wire,
4. thermal lag, and
5. cooling effect of the wire supports.

Neglect of One Velocity Component

It is usually assumed that a slanting wire in the x-y plane is not affected by w (or one in the x-z plane is not affected by v). At any instant in time, however, the flow makes an angle with the x-y plane whose tangent is given by w/U. To evaluate the effect of w, it is pertinent to find the change produced by w on the angle between wire and wind. Denoting by ϕ the instantaneous angle between wire and wind in the x-y plane, by θ the angle equal to $\tan^{-1}\frac{w}{U}$, and by ϕ_i the instantaneous angle between wire and wind in three-dimensional space, it may be shown from geometrical considerations that:

$$\cos \phi_i = \cos \phi \cos \theta$$

A consideration of this equation shows, for $\phi = 45^{\circ}$, that θ must exceed 10° before $\phi_i - \phi$ is greater than 1°. It is the smallness of the change in ϕ that justifies the assumption that the wire is insensitive to the third component of fluctuating velocity. The net effect is a small positive error in signal.

This type of error is applicable only to the $\overline{uw}$ and $\overline{uv}$ probes. In the measurement of v' (or w') the voltage fluctuation produced by the lateral component is not an error source because the two wires of the pair are equally affected and thus, because the instantaneous signals are electronically subtracted before squaring, there is no net effect. There is, however, an adverse effect of u on the measurement of v' (or w'). It arises from the assumption that the instantaneous angle between wire and wind is v/U when actually it is $v/(U \pm u)$. Then:

$$\left(\frac{v}{U}\right)_{meas.} = \frac{v}{U \pm u} \approx \frac{v}{U}\left(1 \mp \frac{u}{U}\right)$$

when $\frac{u}{U}$ is small compared to 1. The RMS valve of the right side of the equation can be approximated by the expression:

$$\frac{v'}{U}\left(1 + \frac{1}{2}\frac{\overline{u^2}}{U^2}\right)$$

which indicates the error in v'/U due to u. If u'/U is 0.3, the measured v'/U is too high by 4-1/2 per cent.

A hot-wire responds only to the normal component of velocity, and thus only one of the lateral components of fluctuating velocity affects the response of a single wire normal to the wind. The error in u'/U arising from the neglect of the normal lateral component is small until the latter becomes quite large. In this event, the type of error to be discussed under "large turbulence fluctuations" becomes so large as to cause the error from this cause to become insignificant.

Large Turbulence Fluctuations

For constant current operation, the basic equation used as a starting point to reduce the hot-wire signals to those having the significance of turbulent quantities may be stated:

$$\frac{R}{R - R_a} = D + F\sqrt{U \sin \phi}$$

where R is the resistance of the hot-wire, R_a is the ambient resistance of the unheated wire, D and F are constants, and ϕ is the angle between wire and wind. This relationship has been well verified by experiment.

The usual extension of this linearized response to apply to the velocity fluctuations requires the assumption that the relative turbulence intensities are small. Computations based on this theory become increasingly inaccurate when the turbulence levels exceed say, 10 per cent.

An analysis of the true response of the hot-wire in the presence of large fluctuations quickly becomes very complex. Hinze, considering only the error in u', derives a lengthly expression for the error by starting from a series expansion for the square root of U. He simplifies his results for the case of isotropic turbulence to show that the linearized theory would give too high a value for u'/U by about 10 per cent when u'/U is 0.2.

Schubauer and Klebanoff, using an approximate analysis based on assumed sinusoidal fluctuations and experimental calibrations of voltage (resistance) against velocity and voltage against angle, considered the effect of large fluctuations on the constants A and B which connect the fluctuating voltage signals to the turbulence quantities. Their results are tabulated below. The errors in the second column apply to the determination of u'/U, and are positive in direction (that is, the measured value is too high). The figures in columns three and four apply to errors in $\overline{uv}$ and $\overline{uw}$, and are the sums of the errors in the two columns for the appropriate values of the turbulence intensities of the components involved in the cross-product. Again, the effect is such as to cause the measured signal to be too high.

These considerations do not apply to the measurement of v' and w'. These quantities are subject to error from this cause only when their amplitude exceeds the linear portion of the calibration curves of voltage-

$\frac{u'}{U}, \frac{v'}{U}, \frac{w'}{U}$	Wire normal to wind	Wire 45° to wind	
	Per cent error in A	Per cent error in A	Per cent error in B
.05	0	0	0
.10	0.2	0	1.0
.15	1.5	1.0	5.0
.20	7.0	5.0	9.0
.25	12.5	9.0	14.0
.30	19.0	15.0	20.0
.35	27.0	20.0	—

difference versus stem angle used in the reduction of the fluctuating voltage signals to intensities. These curves are linear over a range slightly less than 15 degrees on either side of a zero stem angle. Thus, amplitudes as great as, say, tan $13^{\circ} \approx .2$ are free from error from large fluctuations. The amplitudes actually present in the tunnel were considerably less than this value.

The only error related to size in $\frac{v'}{U}$ and $\frac{w'}{U}$ arises from the assumption that the tangent of an angle is equal to its value in radians. This is insignificant for angles up to 15 degrees.

Because the procedure used in the measurement of $\overline{vw}$ is the same as for v' and w', it is assumed that no error in $\overline{vw}$ arises from this cause.

Nonuniform Velocity Distribution Along a Wire

The length selected for a hot-wire usually represents a compromise between somewhat conflicting demands, aerodynamic on the one hand, and structual and strength considerations on the other. It is desirable to use wires which are very short in order to obtain results which apply to

a "point"; however, the temperature distribution along the length of the wire varies greatly owing to the cooling effects of the wire supports if the wire is very short. The temperature distribution can be made more uniform by decreasing the diameter of the wire; the diameter cannot be smaller, however, than that required by strength considerations. Moreover, it is difficult to construct a probe so that its supports do not interfere with the air stream if the wires are very short.

These factors limit the minimum length which a wire may have to about 0.5 mm. (0.020 inch). Longer wires were used in the present study, varying in length from 0.030 inch up to 0.066 inch. Some of the measurements made using these wires are thus subject to some error because of the fact that the velocity distribution along the wire lengths was not uniform.

Wire "length" corrections are usually based on consideration of the correlation between the turbulent fluctuations obtained from two probes as the distance between the two probes is systematically varied. No correlations were measured during the present study, and thus, no length corrections have been applied. The correlation measurements made by Laufer (22), however, in a two-dimensional channel of a similar width, and for the same Reynolds number, indicate these corrections to be of a negligible magnitude in the case of u'. Corrections on the order of from one to about four per cent are perhaps applicable to the measurements of v' and w'; the measurements near the boundary being subject to the larger corrections. The effect of wire length is to cause the measured values of turbulence to be low.

Thermal Lag

Because of finite dimensions of a wire, the temperature fluctuations of the heated wire lag the rapid velocity fluctuations of the air stream. Without compensation, the intensity of the turbulent signal will be measured too low.

In the present work, compensation was provided by an electronic circuit which amplified the higher frequency components of the signal. The magnitude of the adjustment was controlled by a visual comparison of the turbulence signal against a superimposed square wave.

Cooling Effect of the Wire Support

Due to size, the wire supports usually have an infinite heat capacity relative to that of the wire, and the wire is cooled by heat conduction to the supports. This has the effect of reducing the effective length of the wire, and in the case of the very short wire, to cause the temperature distribution along the wire to be very nonuniform. This last situation conflicts with the assumption made in the development of hot-wire theory.

The principal concern arising from this consideration is the necessity for providing sufficient wire length to allow the temperature distribution to become uniform over an appreciable portion of the wire. The minimum length required to attain a reasonably uniform distribution is usually stated to be at least 200 diameters. The wires used during this investigation met and exceeded this requirement.

Mean Velocity Measurements

The mean longitudinal velocity distribution over the test section of the channel was measured by means of a stagnation tube which was used

in conjunction with a floor piezometer. The outside diameter of the stagnation tube was 0.035 inch. A null-type alcohol micromanometer was used to measure pressure differentials.

Pressure Gradient Measurements

The longitudinal pressure gradient was measured from the indications given by the piezometers spaced at one-foot intervals along the channel.

Speed Calibrations

Prior to testing, the motion pattern at the test section was established by reference to a speed-calibration chart. The calibration consisted of the simultaneous measurement of the maximum channel velocity and a reference pressure as the fan speed was systematically varied. The reference pressure was the pressure difference between the settling chamber and the piezometer farthest downstream. The chart was constructed by plotting pressure difference against velocity.

During testing, the motion pattern was maintained constant by repeated reference to a micromanometer which indicated the calibrated pressure difference. The speed calibration served also in the calibration of the hot-wire probes, to be discussed later.

CHAPTER IV

RESULTS AND DISCUSSIONS

Fully Developed Character of the Flow

The theoretical development of Chapter II assumed a channel of sufficient length to permit the establishment of a flow in which variations in the mean values of the velocity and the mean squares of the velocity fluctuations with longitudinal distance are very small.

While adequate criteria for the length necessary to the establishment process are available for flow in pipes, such is not the case for flow in the non-circular conduits. As has already been noted, the length to which the experimental channel of this study could be constructed was limited by the dimensions of the basic tunnel and of its enclosure to a distance of 29 feet.

Measurements by Laufer (22) in the two-dimensional flow region at the downstream end of a shorter channel (23 feet) of similar width and comparable smoothness at approximately the Reynolds number of the present study indicated that the mean velocity did not vary further in the downstream direction. He found, however, that u' was decreasing with x at the centerline of the channel, but concluded that the gradient waa very small as compared with $\frac{1}{\rho}\frac{\partial P}{\partial x}$.

A detailed exploration of the mean velocity field in the 29 foot channel was made with the stagnation tube at a section 22 inches upstream from the end of the channel prior to the installation of the entrance honeycomb. A repetition of the measurements at the downstream measurement

section, and a subsequent comparison of the two sets of data indicated no discernible difference between the two. These measurements were not repeated after the honeycomb was in place. Instead, a series of traverses were made in a direction outward from a vertical boundary to the channel centerline at a distance above the floor equal to three inches at increments of distance along the channel equal to about three feet, starting with $x = -19$ feet. The measurements were made with a 1/4-inch diameter pitot-static tube. The results are shown on Figure 8. Because they are used for exploratory purposes only, no corrections have been applied to the data. The methods used to position the tube with respect to the floor were relatively crude, and some of the small scatter in the results may be due to this cause.

The measurements indicate that the velocity quickly assumes its terminal value near the sidewall. Nearer the centerline, the velocity is initially high, then decreases in a systematic manner. Over the last six feet of the channel, $\partial U/\partial x$ is very small, if not zero.

Corresponding measurements to determine the variation of the turbulence quantities with downstream distance were not made. The mean piezometric pressure distribution along the channel length is shown in Figure 9.

Because of the asymptotic nature of the establishment process, it is probable that a very long channel would be required for complete development. It cannot be concluded that the flow in the test channel is in a state of complete development (see Appendix), and the velocity measurements of this study must be accepted with reserve. It will be shown that the principal finding of this report is not seriously affected by this shortcoming.

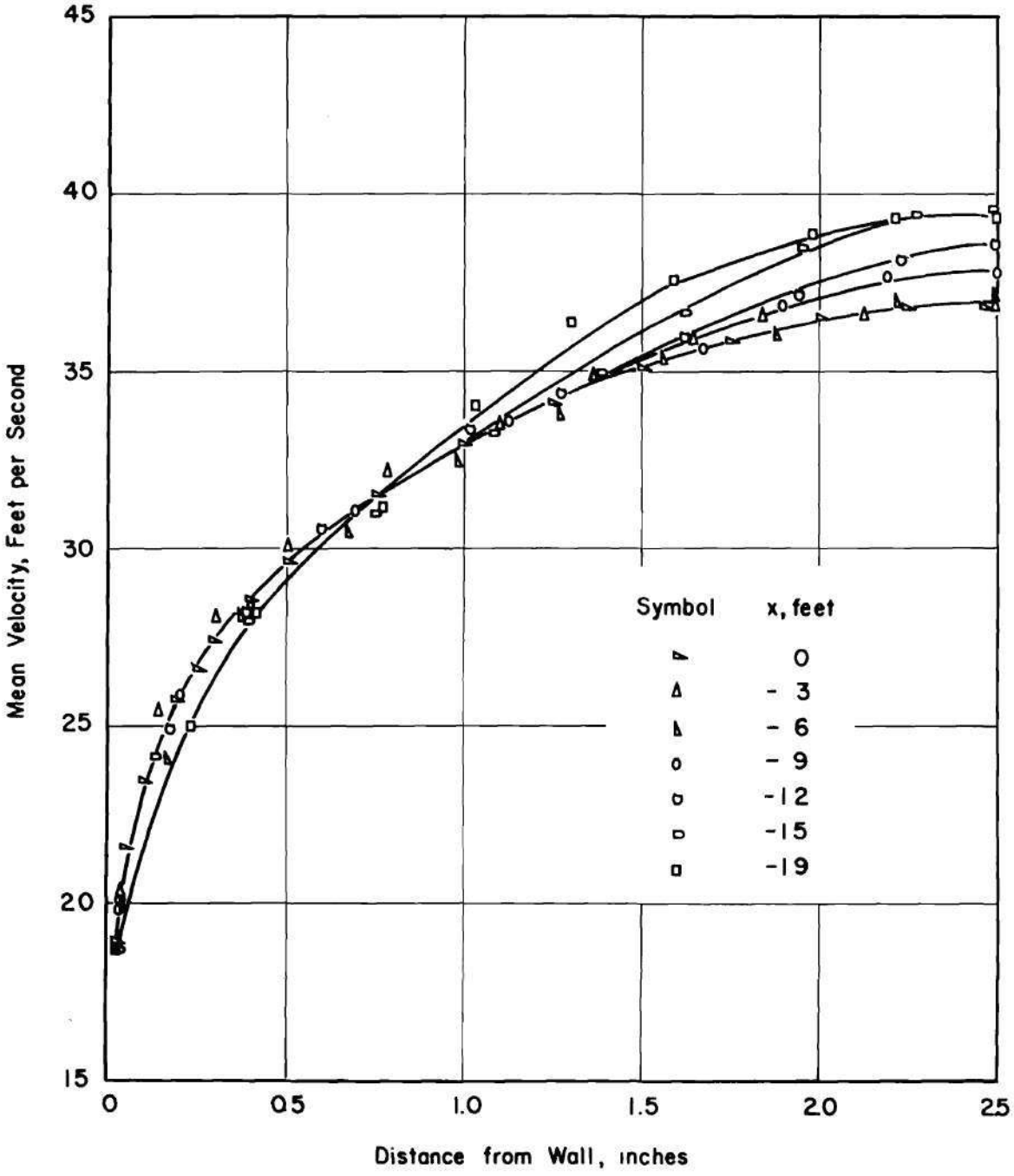

Figure 8. Mean Velocity Distribution at y = 3 inches.

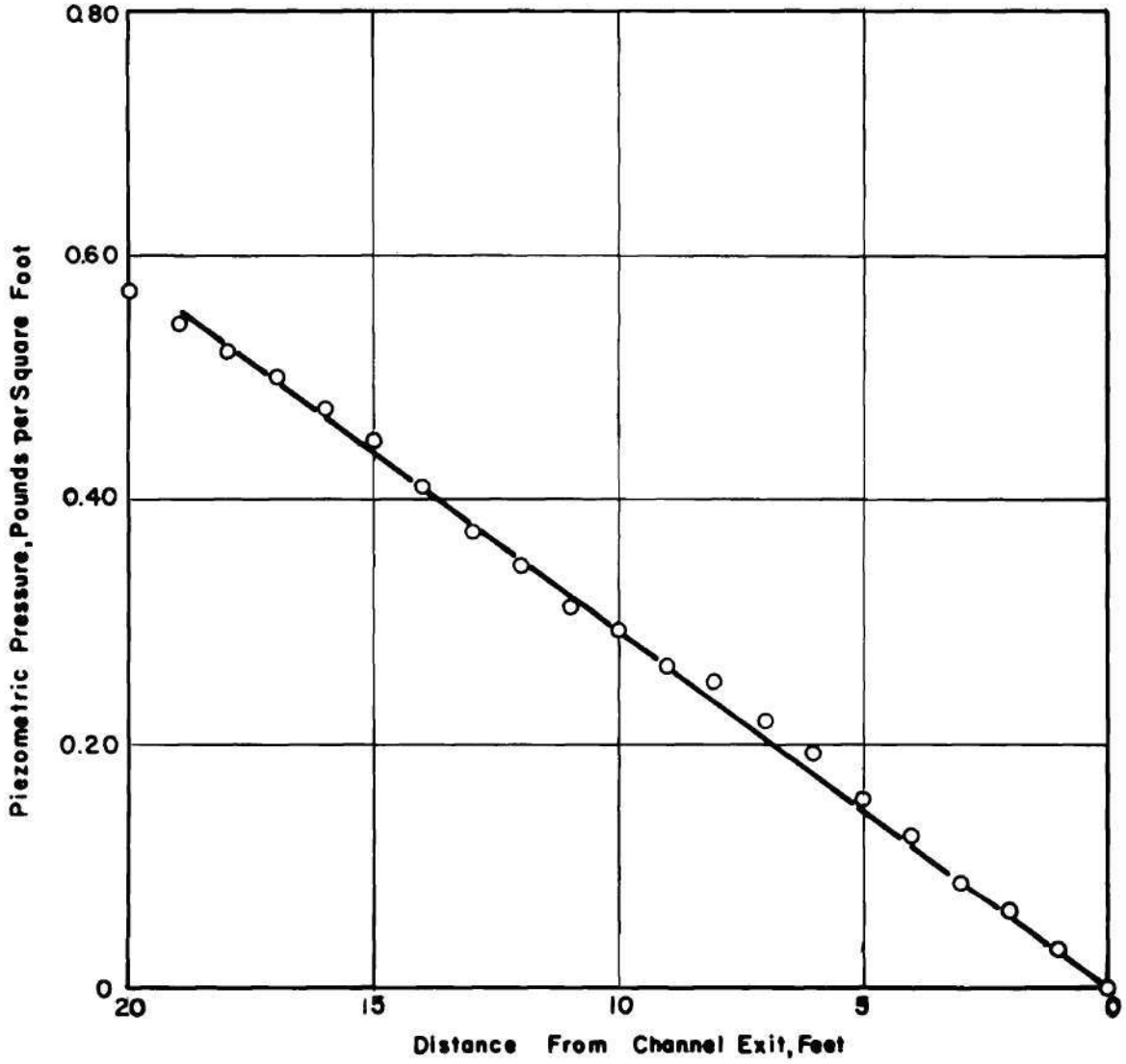

Figure 9. Mean Piezometric Pressure Distribution Along Channel.

Distribution of Mean Velocity

Tedious and time consuming adjustments were made after the installation of the test conduit in order to reduce pressure surges from the system, and to obtain flow symmetry about the horizontal and vertical axes of the conduit. The final measurements indicated that, within one per cent limits, the flow pattern was symmetrical with respect to both axes. The distribution of mean velocity over one quadrant of the channel is shown in Figure 10. For these and all subsequent measurements, the maximum velocity in the two-dimensional region in the central part of the channel was maintained at 40 feet per second.

Figure 10 shows a family of curves, each of which represents a velocity traverse made in the horizontal direction outward from one of the vertical walls of the channel to the channel centerline. Each velocity has been divided by the maximum channel velocity, U_o. The vertical location of each traverse with respect to the channel floor is identified in the legend. The measured velocities have been corrected for the effect of the turbulence fluctuations in accordance with the equation:

$$U_{corr.} = U\sqrt{1 - \frac{\overline{u^2} + \overline{v^2} + \overline{w^2}}{U^2}}$$

The correction from this cause becomes important only very close to a boundary, and has a maximum value of about four per cent. F. A. MacMillan (23) has shown that the effective center of a stagnation tube is displaced from its geometric center toward the region of higher velocity when the velocity distribution across the tube face is not uniform. His experimentally determined correction factors have been used to adjust

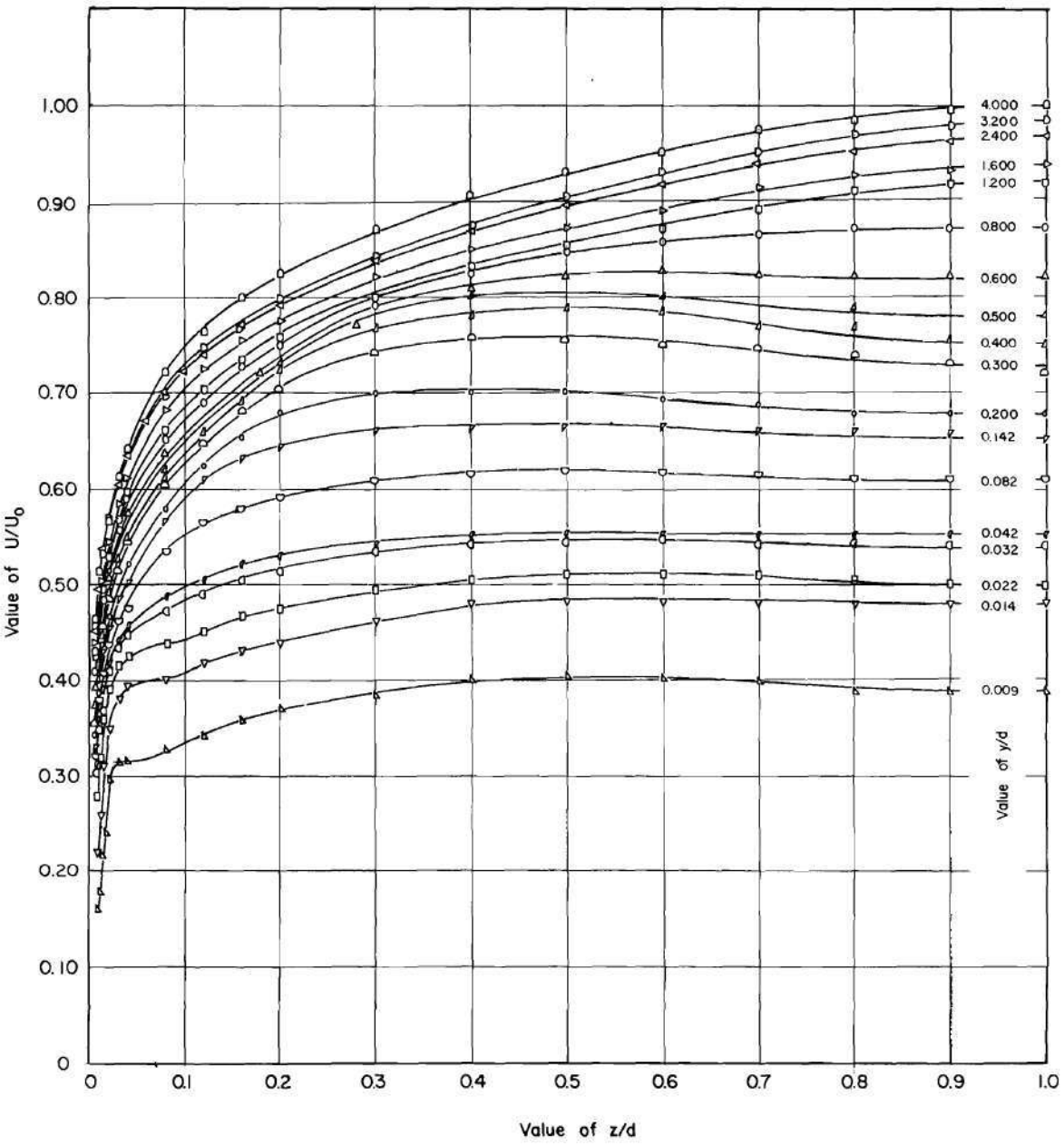

Figure 10. Distribution of Mean Velocity.

the plotting position of the observed velocities. The correction from this source is constant and equal to about 0.005 inch.

At values of y/d greater than about 4(y = 10 inches), and less than about 8.8(y = 22 inches), the measured velocity is independent of the y-coordinate, and the horizontal traverses superpose. While the existence of such a two-dimensional region is to be expected, its limits in this case are probably affected by a lack of complete flow development in the channel. The velocity distribution in this region is logarithmic from the edge of the laminar sublayer to a point close to the horizontal centerline. Between these limits, the distribution of velocity may be represented by the equation:

$$\frac{U}{U_*} = C_1 + C_2 \log \frac{zU_*}{\nu} \tag{16}$$

where U_* is the "local" shear velocity, $\sqrt{\frac{\tau_o}{\rho}}$, $\tau_o = -\frac{d}{\rho}\frac{dP^*}{dx}$, d is the half-channel width, and C_1' and C_2 are constants. The constants are 3.3 and 6.5, respectively. Laufer (22), for a 5-inch channel of larger aspect ratio, obtained coefficients which were equal to 5.5 and 6.9; which, for the same U_*, would indicate higher velocities than those of the present study. This result is a manifestation of the effect of aspect ratio, rather than a measure of the relative smoothness of the two channels, which were perhaps comparable; and simply indicates that the relative part of the total channel occupied by the three-dimensional regions of retarded flow is greater for the channel of smaller height. It is to be remarked that the slope of the logarithmic mean velocity curve (the constant C_2) is larger than that obtained from the experiments of Nikuradse in a circular pipe (C_2 = 5.75).

Below the curve representing the velocity distribution at $y/d = 4$, the mean velocities decrease in a systematic manner. For $4 < y/d \lesssim 1.6$ the profiles are logarithmic; however, the decrease in velocity is relatively greater at the centerline than at the sidewall with decreasing distance from the floor. This has the effect of a decrease in the value of both constants of Equation (16). It is probable, however, that the decreases indicate local changes in wall shear stress (and therefore, in U_*) rather than actual changes in C_1 and C_2.

At the channel centerline, $\frac{\partial U}{\partial z}$ must be equal to zero from conditions of symmetry. At $y/d = 1.2$ the velocity profiles begin to flatten at the centerline to a degree not required by this condition. Below $y/d = 1.2$, the flattening process continues, with an increasingly greater portion of the length of the curve subject to this influence; also, the point at which the velocity attains its maximum value is no longer located at the centerline, but is displaced toward the sidewall to a distance depending upon distance above the floor. While the reversal is apparent in all of the remaining profiles, the difference between the maximum and the centerline velocity is greatest for the profile corresponding to $y/d = 0.4$. Lower in the channel, the magnitude of this difference decreases, and the profile nearest the floor exhibits almost a constant value of velocity for the greater part of its length. Some portion of each velocity traverse is logarithmically distributed throughout the floor-affected region. The part of the curves so described are located next to the sidewall, and are very short for those profiles near the floor.

An almost identical behavior is observed in wall regions of open channels. In the open channel, however, the mean velocity gradient is

not zero at the free surface, and the velocity reversals are more pronounced than in the closed conduit.

Distribution of u'/U and u'/U_o

The measured distribution of u' relative to the local mean velocity over one quadrant of the test section is shown in Figure 11. The measurements are shown in the same manner as for those of the mean velocity -- that is, by a family of curves, each representing a horizontal traverse in a direction outward from the vertical wall to the centerline at a constant distance from the channel floor.

The distribution of $\frac{u'}{U}$ in the central region of the channel has the same general shape as that reported by Laufer (22), Reichart (24), and Laufer (25). The magnitude of the fluctuation has a minimum value at the centerline of the channel, and increases slowly in a direction toward the wall. Near the wall, the rate of increase is very rapid. Although detailed explorations very close to the wall were not made, the measurements suffice to indicate that the maximum value of $\frac{u'}{U}$ occurs within the laminar layer ($\delta \approx .03$ inch); which is in accord with Laufer's (22, 25) results both in a channel and a pipe. It has already been noted that the response of a hot wire for large fluctuations errs toward higher values of the fluctuations than are actually present, so that the magnitude of $\frac{u'}{U}$ very close to the wall must be regarded as approximate.

Laufer (22) indicates that the magnitude of the velocity fluctuations decreases slowly with increasing Reynolds number. At comparable Reynolds numbers, and except close to the wall, the measured values of u'/U are slightly greater than those measured by Laufer in a channel, which is perhaps due to slight differences in equipment and techniques.

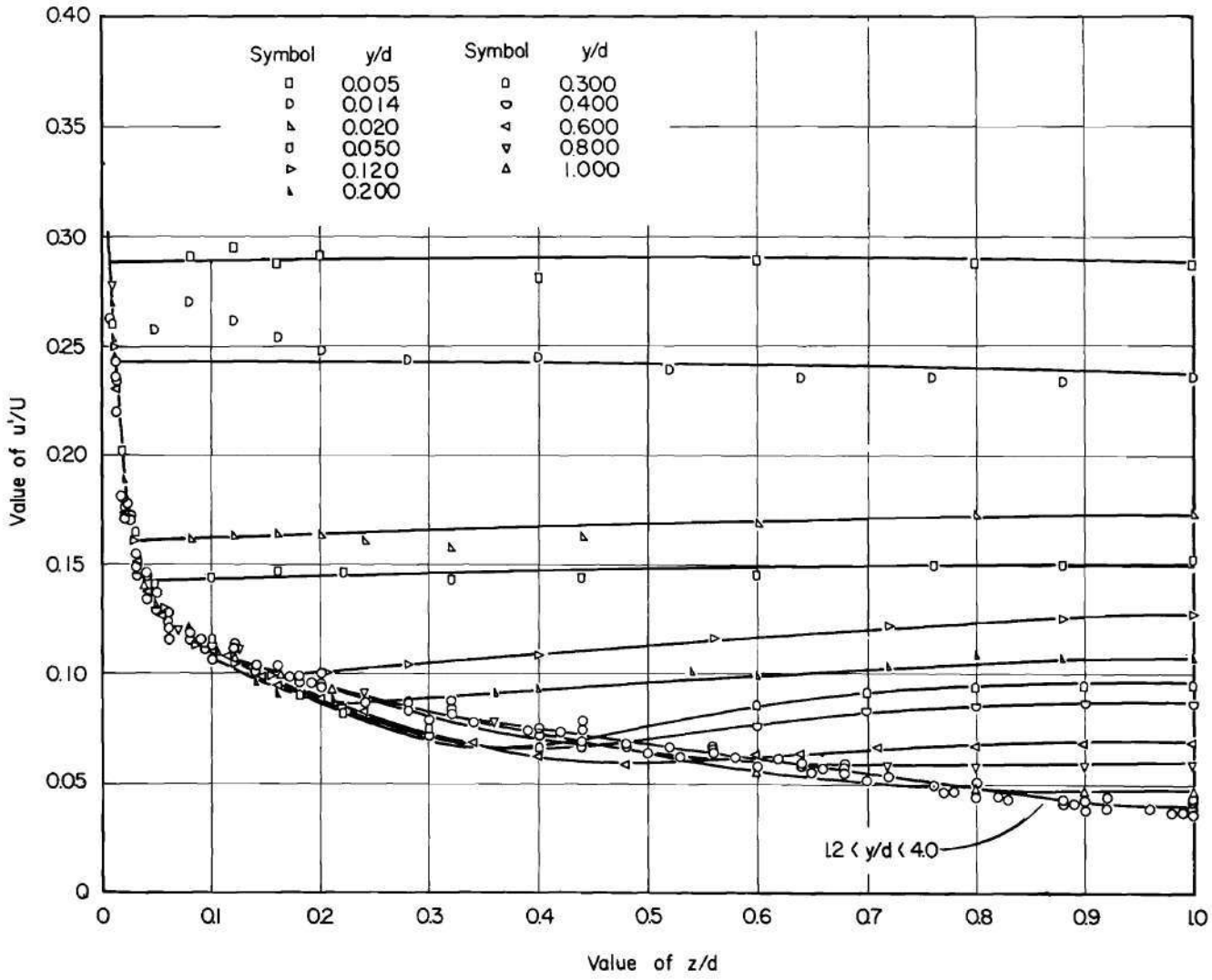

Figure 11. Distribution of Velocity Fluctuation u' Relative to Local Mean Velocity.

Below $y/d = 4$ and above $y/d \approx 1.2$, the transverse distributions of u'/U superpose upon the curve representing the central region (that for $y/d = 4$). Turbulence measurements were not made above a height of 10 inches in the channel. Because the transverse turbulence profiles superpose between the limits noted above, and because the corresponding mean velocities decrease, it follows that over this region the absolute magnitudes of the turbulent fluctuations increase in the ratio to which the velocities decrease.

Below $y/d \approx 1.2$, and away from the wall, the transverse distributions of $\frac{u'}{U}$ diverge from the single curve representing this quantity above this height. The gradients of the curves are almost the inverse of those of the corresponding curves representing the distribution of mean velocity. Whereas the latter curves have maximum values between the centerline and the wall, the $\frac{u'}{U}$ distributions have minimums, although the location of the points in the two cases are only approximately coincident. Both sets of curves have a zero gradient at the centerline. At the sidewall, the curves of u'/U superpose, irrespective of distance above the floor. Away from the sidewall, in general, the magnitude of $\frac{u'}{U}$ increases with decreasing y.

The variation of u' relative to the maximum mean velocity in the channel, U_o, is shown in Figure 12 for y/d equal to or less than 1.2. It may be observed from the figure that the magnitude of u'/U_o, and therefore of u', at a given distance from a boundary, is the same, to a good approximation, whether the orientation of the boundary is horizontal or theoretical.

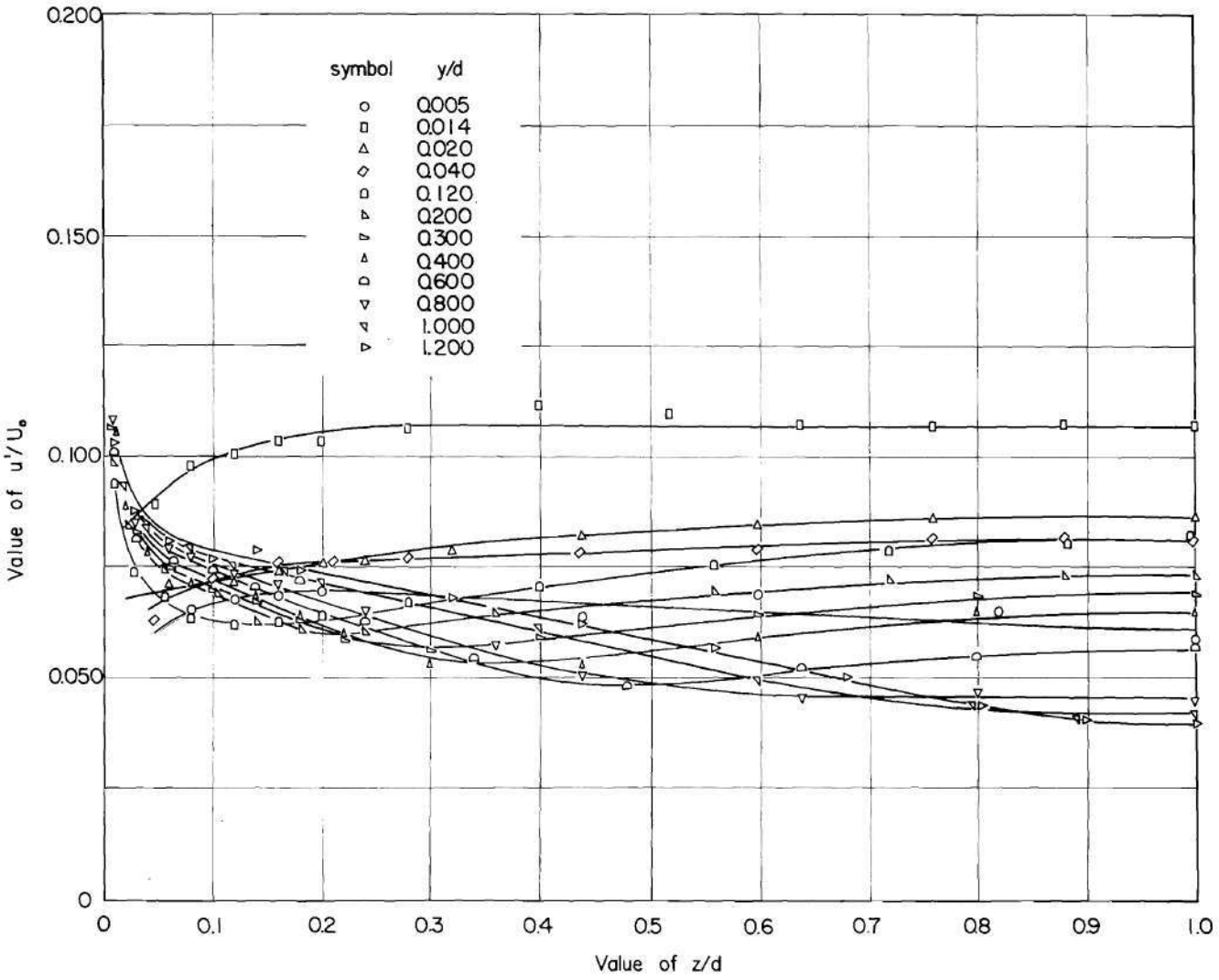

Figure 12. Distribution of Velocity Fluctuation u' Relative to Maximum Mean Velocity.

Distribution of $\frac{v'}{U}$ and $\frac{v'}{U_o}$

The measured values of $\frac{v'}{U}$ over one quadrant of the normal section are shown in Figure 13 for values of y/d equal to and less than 1.2. The manner of representation is the same as for the distributions of U, u'/U, and u'/U_o already shown.

For y/d greater than 1.2, and except in the immediate vicinity of the centerline, the horizontal profiles superpose on the curve which represents the measurements at a height of three inches. Because of the relatively greater scatter in the values of $\frac{v'}{U}$ (in contrast to those of $\frac{u'}{U}$), which would obscure the variation of the plotted points, the latter measurements are not shown. At the centerline, the value of $\frac{v'}{U}$ decreases slightly between y/d = 1.2 and y/d = 4.0. The portion of the traverse for y/d = 4.0 which differs from that for y/d = 1.2 is shown in Figure 13 as a dashed line.

The curves of $\frac{v'}{U}$ display the same general trends as those already noted for those of $\frac{u'}{U}$, differing only in two major aspects. At the centerline, away from the floor-affected region, the numerical magnitude of the two fluctuations are almost equal, that of u' being slightly higher. In the direction of fixed boundary, the rate of increase of $\frac{v'}{U}$ is much smaller than the corresponding rate of increase in $\frac{u'}{U}$, and consequently, at the boundaries, $\frac{u'}{U}$ is several times greater than $\frac{v'}{U}$. The second difference in the two distributions is the "lopsided" appearance of that of $\frac{v'}{U}$, resulting from a greater rate of increase in $\frac{v'}{U}$ in a direction toward the vertical boundary than in a direction toward the floor. The variation of v'/U_o for y/d equal to and less than 1.2 is shown in Figure 14.

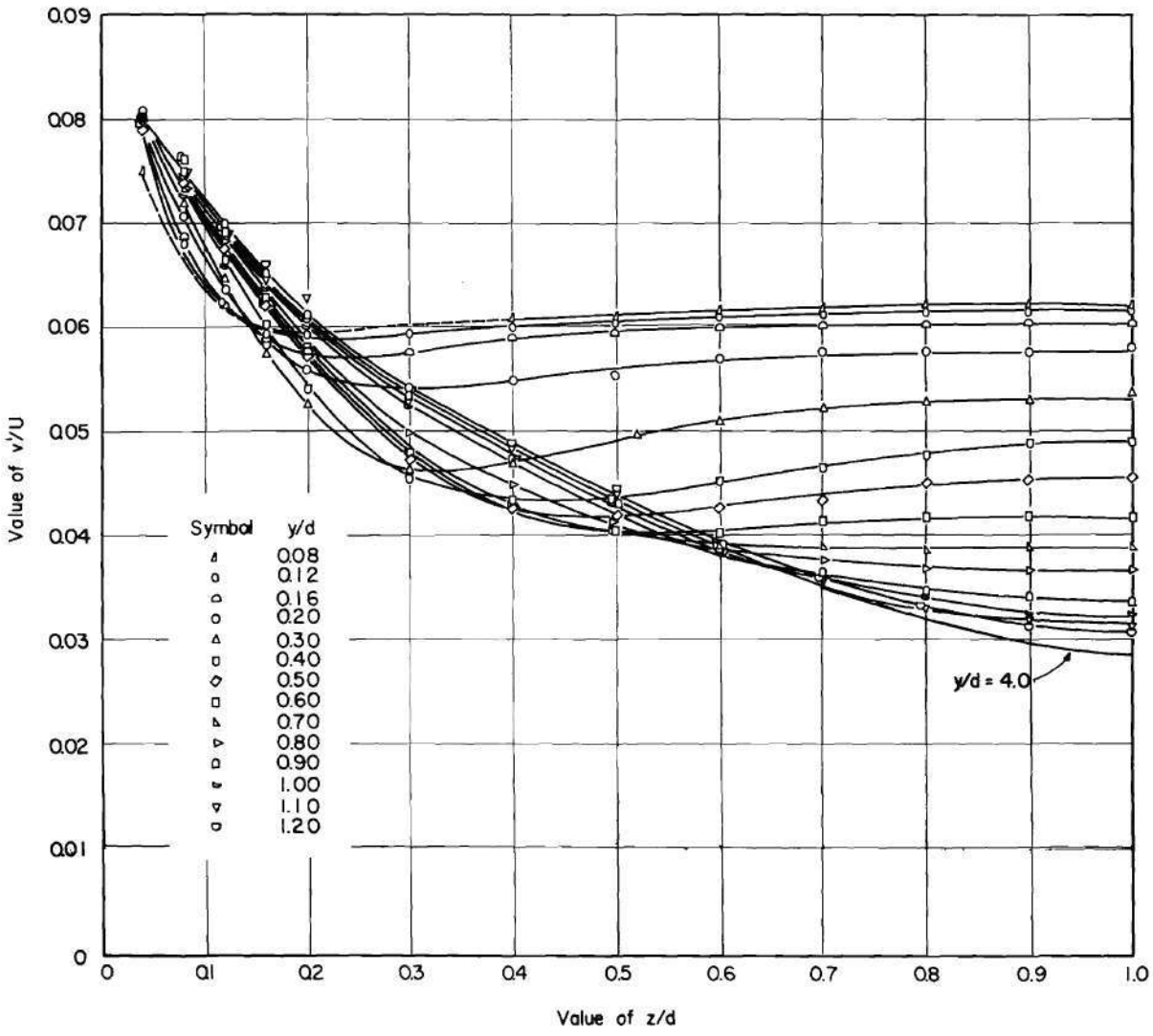

Figure 13. Distributions of Velocity Fluctuation v' Relative to Local Mean Velocity.

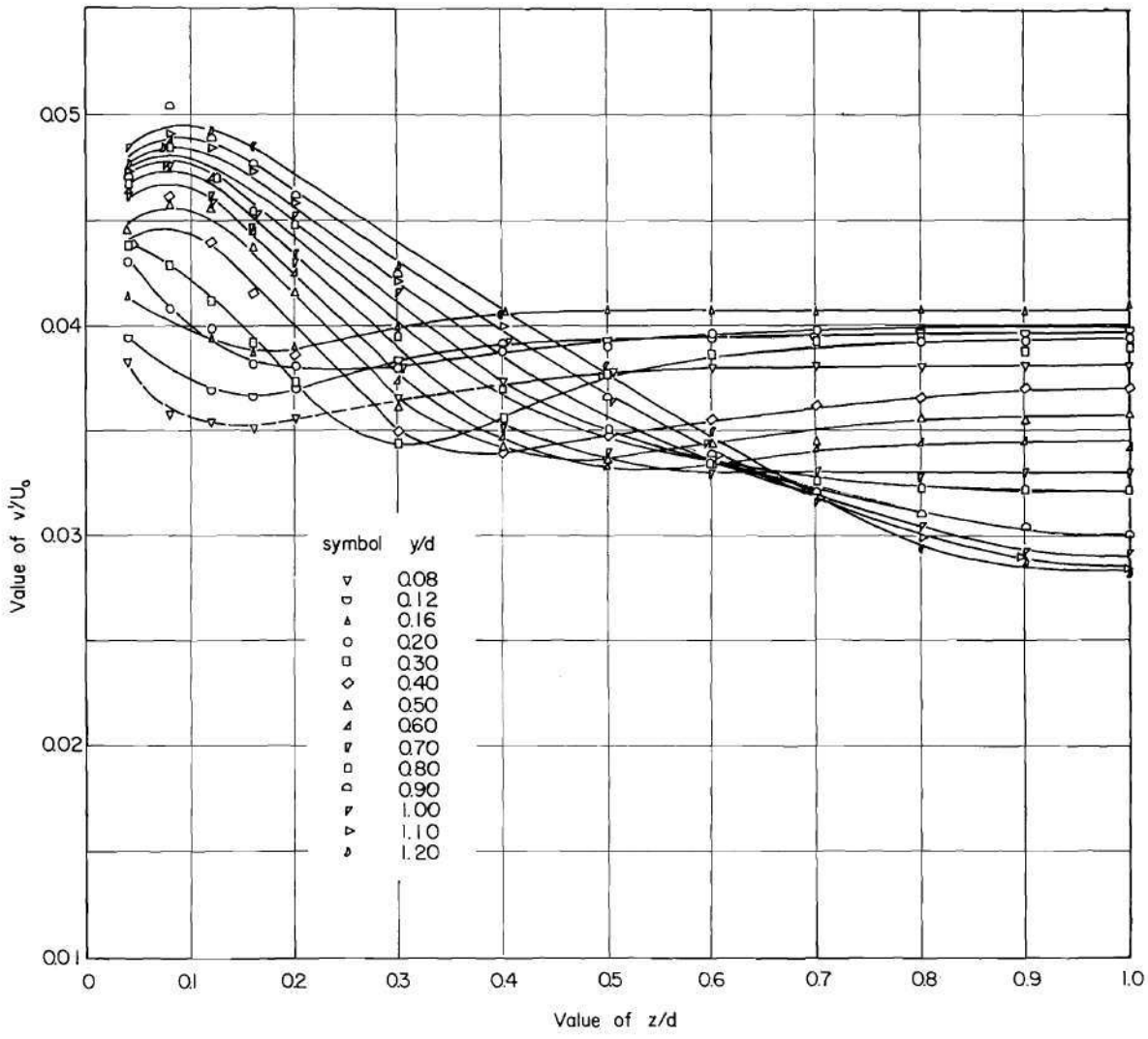

Figure 14. Distribution of Velocity Fluctuation v' Relative to Maximum Mean Velocity.

Distribution of $\frac{w'}{U}$ and $\frac{w'}{U_o}$

The distribution of $\frac{w'}{U}$ over one quadrant of the channel is shown in Figure 15. As for $\frac{v'}{U}$, the traverse profiles superpose in the channel above y/d = 1.2. The portion of the traverse for y/d = 4 which is different from that at y/d = 1.2 is shown as a dashed curve.

The values of $\frac{w'}{U}$ are of the same order of magnitude as those of v'/U, except near a boundary. Whereas $\frac{v'}{U}$ has its greater value near the vertical boundary, and a smaller value near the horizontal boundary, exactly the reverse is true for the case of $\frac{w'}{U}$. Indeed, except for small local variations in the regions where the reversals in mean velocity occur, a cross plot of w'/U may be almost exactly superposed on the transverse distributions of $\frac{v'}{U}$ shown in Figure 13. The variation of w'/U_o for y/d equal to and less than 1.2 is shown in Figure 16.

Distribution of $\overline{uv}$

Inherently, the average cross-products of the fluctuating components are less susceptible to precise measurement than the quantities u', v', and w'. Each of the former involves a difference between two average signals whereas the latter depends only upon one time-averaged response. When the signals are of approximately the same order of magnitude, the combined error may be larger than the resultant difference to which the cross-product is related.

The quantity $\overline{uv}$, upon multiplication by ρ, may be interpreted as the transport of x-momentum through a surface normal to the y-axis. It has the dimensions of force per unit of area, and has the significance of a shear stress. The distribution of $\overline{uv}$ relative to U_*^2 is shown in Figure 17

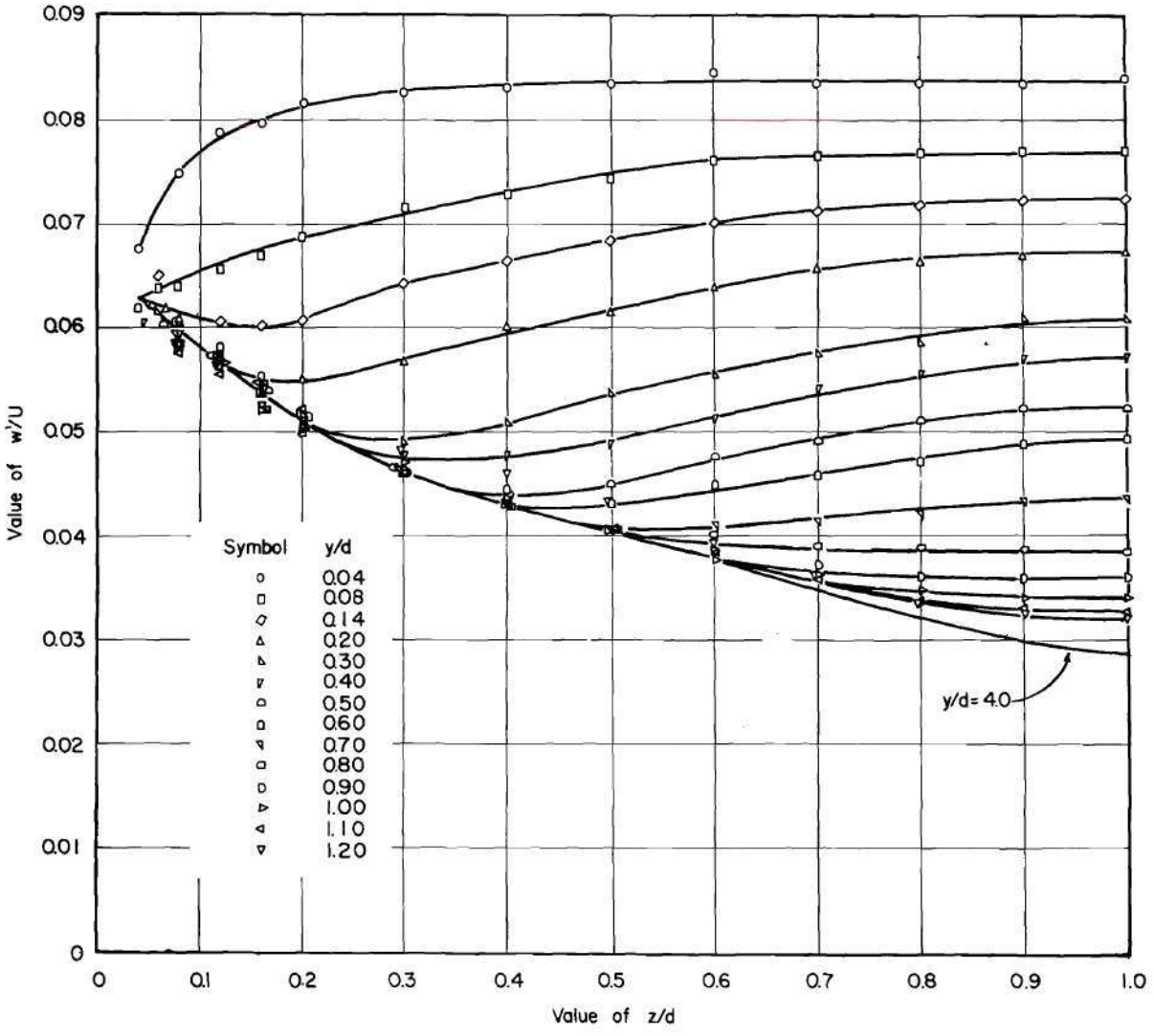

Figure 15. Distribution of Velocity Fluctuation w' Relative to Local Mean Velocity.

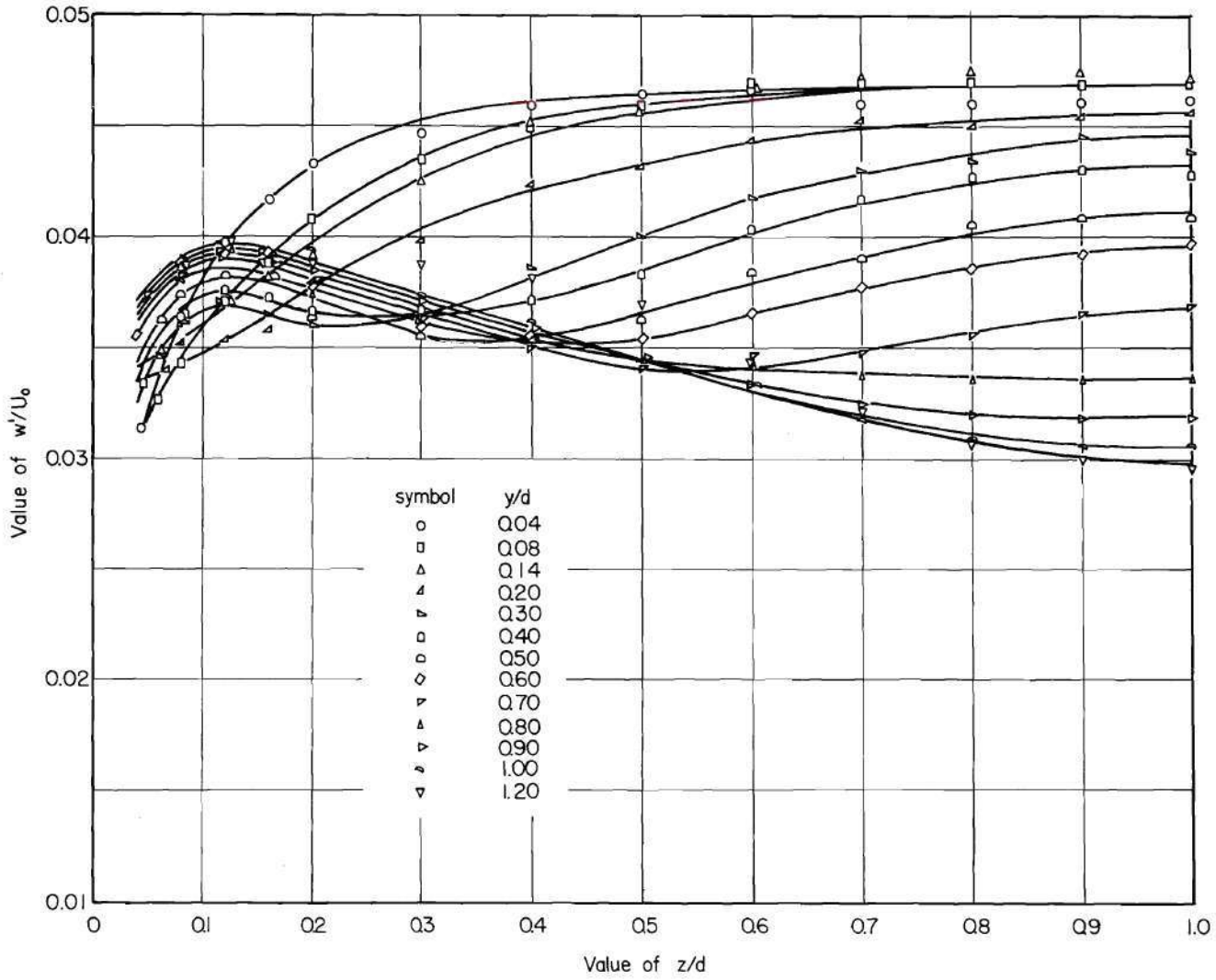

Figure 16. Distribution of Velocity Fluctuation w' Relative to Maximum Mean Velocity.

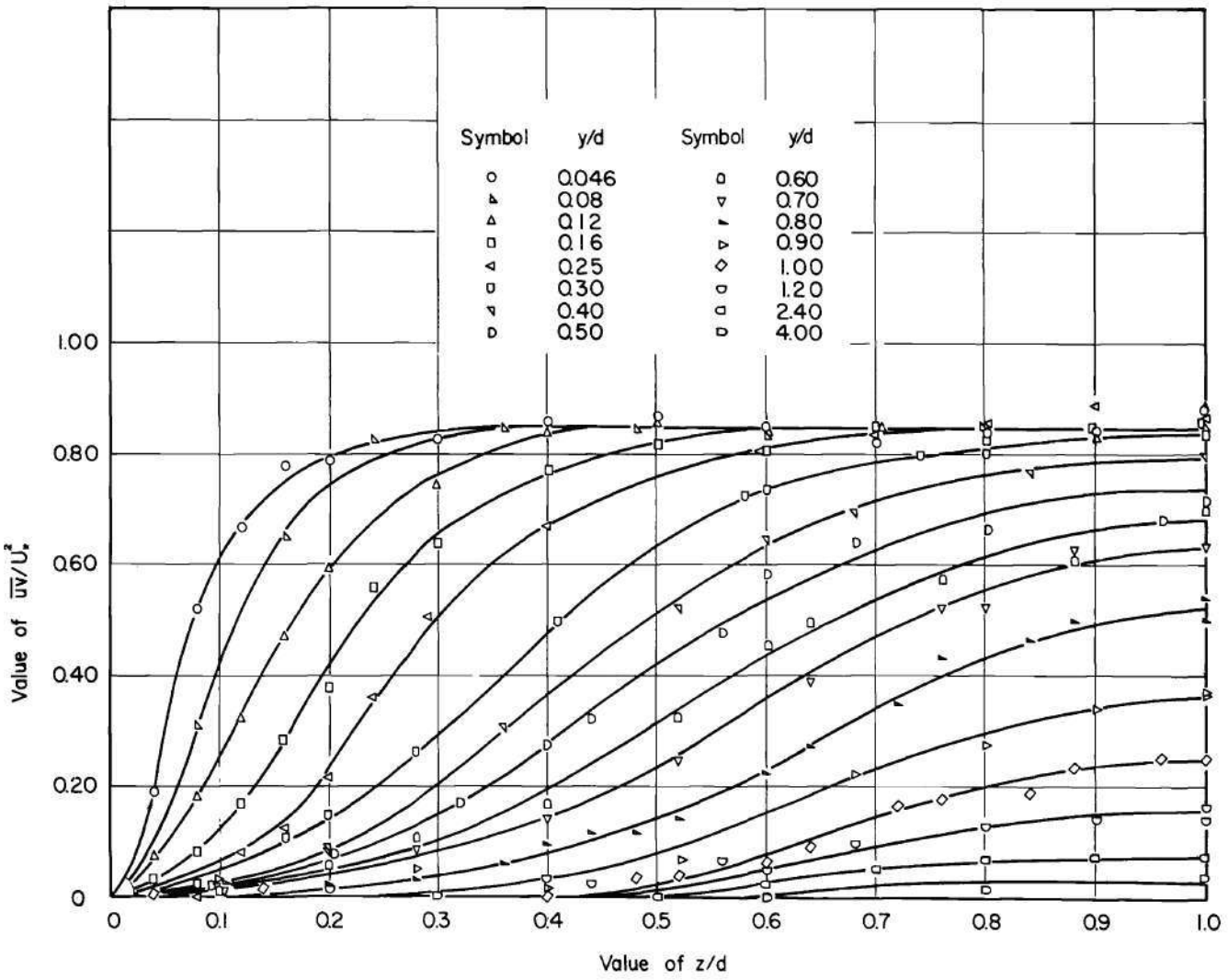

Figure 17. Distribution of $\overline{uv}$.

for one quadrant of the channel. As predicted by the simplified equations of motion, $\overline{uv}$ is zero in the central region of flow. Nearer the floor, the product first has a finite value at the centerline of the channel, and the centerline value increases with decreasing distance from the floor. In the direction toward the sidewall from the centerline, the value of $\overline{uv}$ decreases from that measured at the centerline. The location of the point at which the decrease begins is a function of distance from the floor. At the wall, $\overline{uv}$ is zero throughout. The distribution reflects the dependency of $\overline{uv}$ upon the mean velocity gradient dU/dy.

The values of $\overline{uv}/U_*^2$ near the floor are smaller than unity by a considerable amount, which indicates that the shear stress at the floor is probably smaller than that on the sidewall in the central region of flow. The smaller values of $\overline{uv}$ are the results of flattened vertical mean velocity profiles due to the reversal in the mean velocity distribution shown in Figure 10.

Distribution of $\overline{uw}$

The quantity $\overline{uw}$, multiplied by ρ, is the transport of x-momentum through a surface normal to the z-axis, and like $\rho\,\overline{uv}$, is an "apparent" shear. The distribution of $\overline{uw}$, relative to U_*^2, is shown in Figure 18. Over one quadrant of the section, within the limits of experimental accuracy, the profiles superpose for y/d greater than about 1.2. The straight line drawn through the points is the variation of τ/ρ computed from the measured longitudinal pressure gradient, independent of the measurements of turbulence. The extrapolated value of the line at the wall is unity.

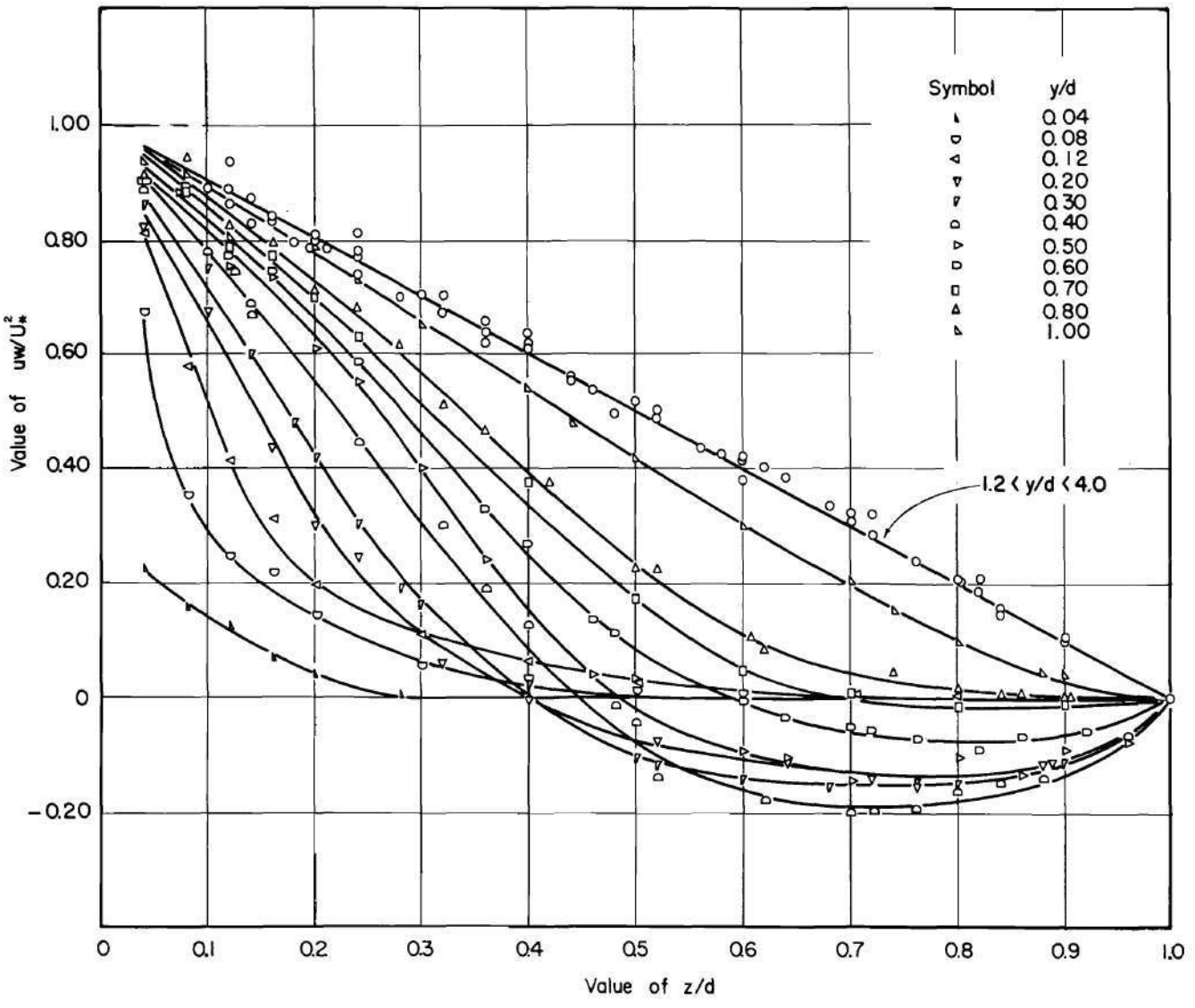

Figure 18. Distribution of $\overline{uw}$.

The value of $\overline{uw}$ is zero at the center of the channel for reasons of symmetry, regardless of position with respect to the floor. Unlike the other distributions shown, it is not required that the gradient of this quantity be zero at the centerline. Below y/d = 1.2 (as well as above), dependency of the value of $\overline{uw}$ on the mean velocity gradient $\frac{\partial U}{\partial z}$ is demonstrated. Thus, as the mean velocity profiles flatten near the centerline, the value of $\overline{uw}$ is shown to decrease. At the points of mean velocity reversal away from the centerline, $\overline{uw}$ is zero, and is negative in sign over the distance that $\frac{\partial U}{\partial z}$ is negative. At the centerline, as $\frac{\partial U}{\partial z}$ is again zero, the value of $\overline{uw}$ increases to zero. At the wall, in contrast, the mean velocity gradient is little affected by presence of the floor, and $\overline{uw}$ decreases only slightly with decreasing distance from the floor until the traverse is located very close to the floor.

Distribution of $\overline{vw}$

The measurements of $\overline{vw}$ were made in accordance with the procedure outlined in Chapter III, and depend upon the detection of a small difference between two large signals of almost equal magnitude. The values of $\overline{vw}$ are small enough to be influenced by experimental error in the component measurements to such a degree that almost no confidence can be placed in the results. The distribution of $\overline{vw}$, relative to U_*^2, over the lower three inches of the channel is shown without comment on Figure 19 for the purpose of indicating the probable order of magnitude of this quantity.

Variation of $(v^2 - w^2)$

While all of the distributions shown in Figures 10 through 20 are necessary to a description of the mean and the turbulent motion pattern

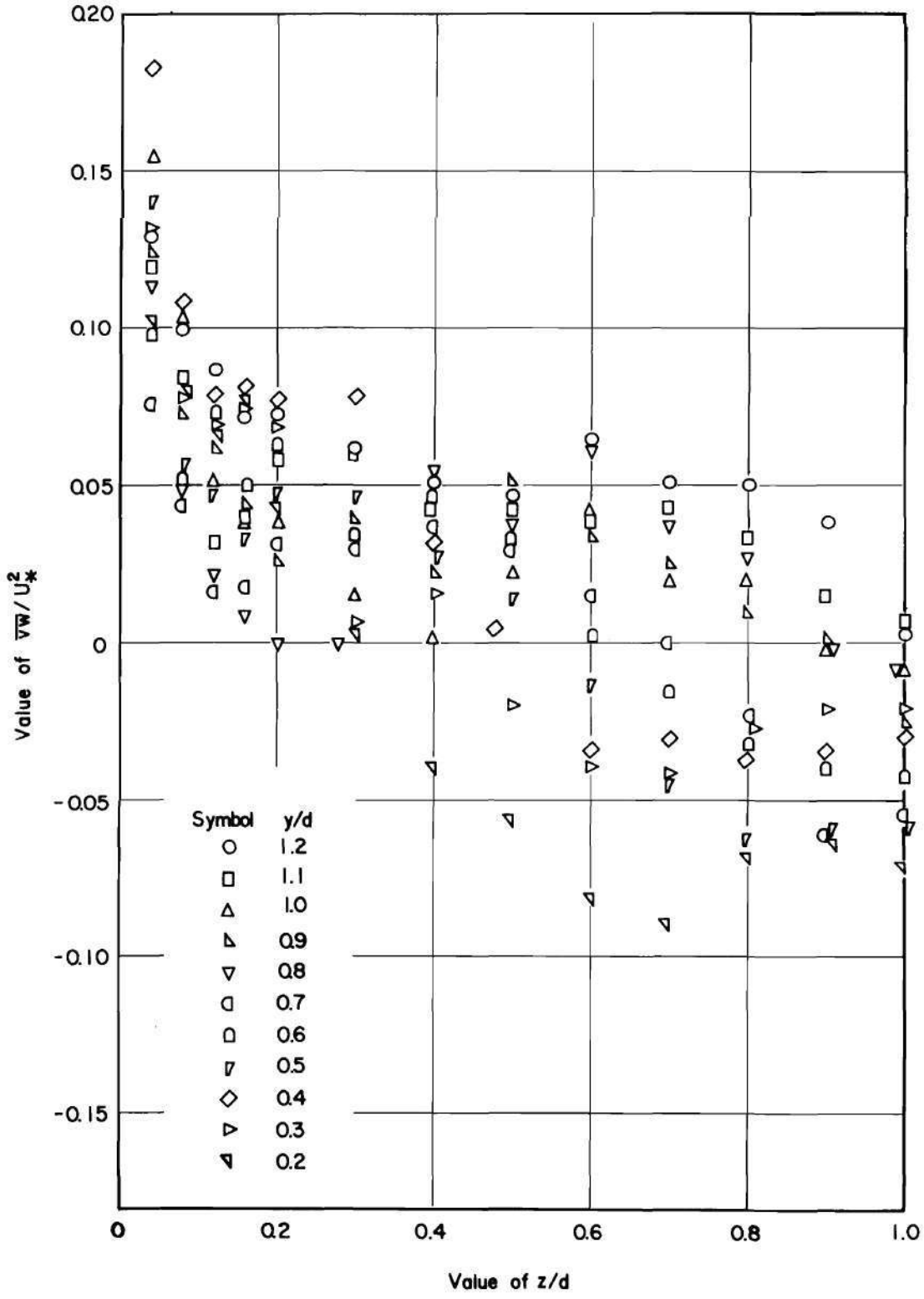

Figure 19. Distribution of $\overline{vw}$.

in the test conduit, those of v' and w' are of particular significance in connection with the secondary motions in the channel. In what follows, the measured distribution of the quantity $(\overline{v^2} - \overline{w^2})$ over the lower part of the channel will first be shown. Next, because the state of development of the flow is to some degree uncertain, and because only the general trends shown by the distribution are important to the later discussion of the secondary motion, the configuration of the curves drawn from the measured data will be shown to be consistent with those expected from a fully established, uniform motion. Finally, the variation of the last term of Equation (13):

$$\frac{\partial^2}{\partial y \partial z} (\overline{v^2} - \overline{w^2})$$

will be generalized from the distribution, and interpreted by the use of Equation (13).

The distribution of $(\overline{v^2} - \overline{w^2})$ for y/d equal to and less than 1.2 is shown on Figure 20. The principal feature to be noted from the figure is the flattening of each curve in the central part of the channel with decreasing distance from the floor, with a corresponding increase in slope nearer the sidewall. This behavior is related primarily to the effect of boundary geometry on the two fluctuating quantities involved, and is readily explainable in terms of this factor. This is most easily shown by a discussion of only the uppermost and lowermost of the curves of the figure with the tacit assumption that the transition from one to the other takes place gradually, and in the manner indicated by the intervening curves on the figure.

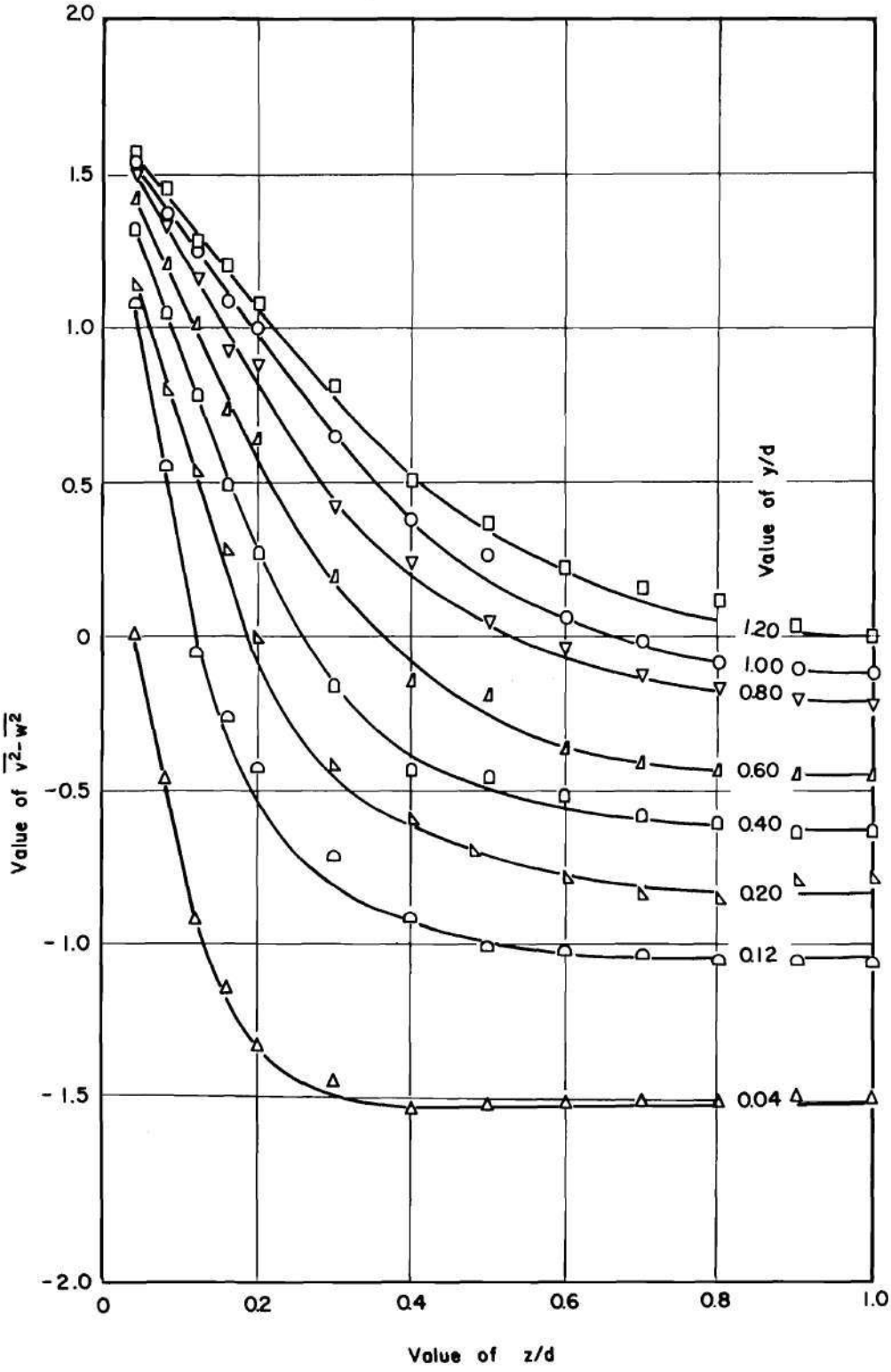

Figure 20. Variation of $\overline{v^2} - \overline{w^2}$.

1. For the uppermost curve (for y/d = 1.2), at the channel centerline, $\overline{v^2}$ is equal to $\overline{w^2}$, and the difference between the two quantities is zero. The strong tendency toward isotropy at locations sufficiently far away from a boundary in closed conduit flow is apparent in the results of other investigations; notably by Laufer, both in a rectangular channel (22) and a pipe, (25) and by Fage and Townend (26) in a pipe.

2. For the uppermost curve, and at the sidewall, $\overline{v^2}$ is greater than $\overline{w^2}$. On the other hand, for the lowermost curve, and away from the sidewall, $\overline{w^2}$ is greater than $\overline{v^2}$. The difference, in each location, is of approximately the same absolute magnitude. The two occurrences are obviously related, and each is explainable by the assumption that, close to a boundary, the larger scale components of a fluctuation normal to the boundary are inhibited by the presence of the boundary, whereas the similar components of the fluctuation parallel to the boundary are allowed to oscillate freely. General substantiation of this assumption is available from other measurements close to a boundary. Laufer (22, 25), for example, for a two-dimensional channel flow, shows that the vertical component of the velocity fluctuations is greater than the horizontal component near a vertical boundary; and for a pipe, that the tangential component of fluctuation is greater than the radial component. Moreover, measurements of the spectrum of v' and w' near the boundary in a pipe by Laufer (25) show that the radial component of fluctuation is deficient in energy at the low frequency end of the spectrum in comparison to the same frequency range in the energy spectrum for the tangential fluctuations. The conclusion concerning the relative magnitude of the two components is further strengthened by the measurements of Fage and Townend (26) in a pipe.

3. Near the floor, except in the immediate vicinity of the sidewall, the motion is dominated by the floor, and the sidewall has little influence. Both the mean and the turbulent components of the flow have almost constant values over the width of the channel in this location, and the value of $(\overline{v^2} - \overline{w^2})$ is practically constant for the greater part of the lowermost curve.

4. At a point equidistant from both the floor and the sidewall, and very close to each, $\overline{v^2}$ is equal to $\overline{w^2}$, and the difference is zero. This circumstance is justified from symmetry considerations.

5. The uppermost curve has an easy curvature throughout its length. This is evident from a consideration of the shape of the individual curves of $\overline{v^2}$ and $\overline{w^2}$, which, in turn, are similar to those measured by other investigations in a two-dimensional or axially-symmetric flow, and is a demonstration of the gradually diminishing influence of a boundary with increasing distance from the boundary.

No claims are made relative to the applicability of the numerical values shown on Figure 20 to a fully established motion. On the other hand, it is re-emphasized that the general shape of the family of curves is a result, primarily, of the effect of boundary geometry, and it is not to be expected that the configuration of a similar set of curves defined from results obtainable in a longer channel would be substantially different from those of Figure 20.

In view of the foregoing, and in conjunction with Equation (13), it can almost immediately be concluded from Figure 20 that secondary motions will exist in the vicinity of a corner in a fully established, turbulent motion. Thus, the gradient $\frac{\partial}{\partial z}(\overline{v^2} - \overline{w^2})$ is proportional (the dimension z

in Figure 20 has been divided by the constant, d) to the slope of the curves drawn on Figure 20. In turn, the rate of change of this gradient with respect to y is the last term of Equation (13), and can only be zero if the slope of the curves is independent of y. Because, except at the centerline, the slopes obviously are a function of y, the latter condition is not obtained, and therefore the second derivative does exist. Equation (13) thus requires that V or W, or both, have values other than zero where the curves are not parallel.

The fact that the second derivative is equal to zero at the centerline does not preclude, either from Equation (13), or from physical considerations, a secondary motion at this location. The equation of continuity requires that the streamlines of the secondary motion close upon themselves; thus, though the motion does not originate there, it may be carried into other regions. Equation (13), on the other hand, may be satisfied by a balance between the terms on the left side and the first two on the right side.

Measurement of Secondary Motion

While the foregoing is useful for the purpose of establishing a reason for the occurrence of secondary motion, it does little to reveal the motion pattern. The vertical and horizontal components of the motion over the lower three inches of the channel were measured by a procedure which utilized the directional sensitivity of a v' probe. The essentials of the method have already been described.

During the measurements, it was realized that the signals which were proportional to the secondary velocities were small enough to be affected to a significant degree by small changes in the response characteristics

of the wires with time. To remove the effect of this variation, the data for each horizontal traverse across the half channel has been separately adjusted on the assumption the wire response remained stable for the period of time required to complete the traverse, which is to assume that relative differences in velocity were correctly measured along each traverse. For each V-traverse, a datum plane was so selected to result in a velocity profile that satisfied continuity requirements across the plane (that is, upward flow equal to downward flow). A continuity basis for the adjustment of the W-traverses is not available, since data was collected only below $y/d = 1.2$. The latter profiles were therefore adjusted to the requirement that W be equal to zero at the center of the channel.

The adjusted data for both V and W have been combined vectorially and plotted on Figure 21. The untipped end of each vector represents the point to which each resultant velocity pertains. A reference vector of length $0.025\ U_o$ (1 foot per second) is shown at the top of the figure. Despite the fact that the corrections detract from claims relative to accuracy, it is believed that the pattern shown on the figure represents closely the true state of affairs. A striking feature of these measurements is the smallness of the motions which they represent. They follow somewhat the general pattern first suggested by Prandtl.

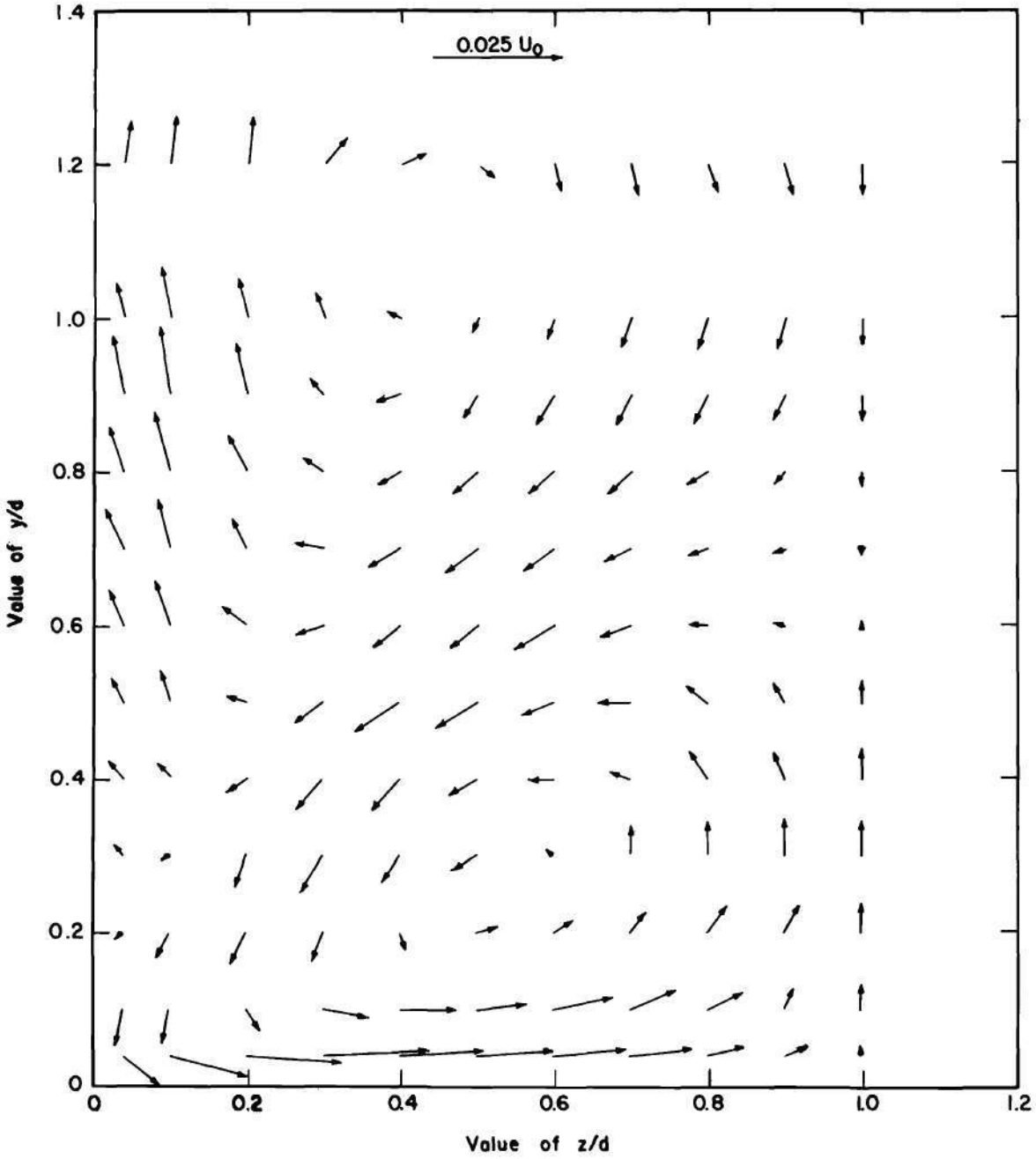

Figure 21. Secondary Velocity Vectors.

CHAPTER V

CONCLUSIONS

The motion pattern for uniform flow in a corner of a non-symmetrical closed conduit is not subject to complete mathematical analysis, because of the difficulties involved in the solution of the non-linear, partial-differential equations of motion. Measurements of the motion pattern, both mean and turbulent, over a normal section at the downstream end of a channel 5 inches in width and 32 inches in height are presented in this report. The applicability of the results to a description of a fully developed flow is uncertain, because of the limited length of channel available for development, which was 29 feet.

The conclusions drawn in this report are:

1. The flow was symmetrical with respect to both the horizontal and the vertical centerlines of the channel. In the vertical direction, the channel was divided into three parts: a central region and two wall regions.

2. In the central region, the distribution of mean velocity was logarithmic from a point very close to the sidewall outward nearly to the vertical centerline, and was independent of vertical position. The root-mean-squares of the fluctuating components, u', v', and w' had maximum values close to the sidewall, and minimum values at the vertical centerline. The magnitude of the three components was nearly the same at the vertical centerline; whereas at the sidewall, u' is largest, and w' the smallest. The quantities $\overline{uv}$ and $\overline{vw}$ were zero throughout the

central region, as were V and W. The cross-product $\overline{uw}$ had a maximum value close to the sidewall; a zero value at the centerline, and was linearly distributed between these two points.

3. In the wall regions, the values of u', v', and w' increased with decreasing distance from the upper and lower boundaries; while the value of U decreased. Close to the boundary, u' was again larger than either v' or w'; however, w' was greater than v'. The variation of $\overline{uv}$ and $\overline{uw}$ was dependent upon the velocity gradients $\frac{dU}{dy}$ and $\frac{dU}{dz}$, and the variation of $\overline{vw}$ upon a gradient in V, or W, or both. The maximum values of $\overline{vw}$ were much smaller than those of $\overline{uv}$ and $\overline{uw}$.

4. Secondary motions are present in long channels of non-circular shape. One of the boundaries may be a free surface.

5. The behavior of the fluctuating components v' and w' are of primary importance to the establishment of the secondary motion pattern in long channels. For a given discharge and surface roughness, the configuration of the boundaries control the magnitude of v' and w'.

6. The magnitude of a velocity fluctuation normal to a boundary is inhibited by the proximity of the boundary. This causes the value of v' next to a vertical boundary to be larger than the corresponding value of w'; and conversely, next to a horizontal boundary, the value of w' to be greater than that of v'. This circumstance, together with Equation (13), can be used to show that a secondary motion will be generated in the vicinity of a corner formed by the intersection of two plane boundaries.

7. The measurements of the secondary motion show that it is directed inward approximately to the corners, and outward from the corners along the boundaries.

8. The results concerning the secondary motions are not immediately applicable to natural stream channels where local changes in channel alignment and shape may cause secondary motions.

CHAPTER VI

RECOMMENDATIONS

The study which this report represents was of an exploratory and preliminary nature. Foremost among the questions which were raised during and after the completion of the experimental work is one of the effect of the length of the channel on the magnitude of the turbulence quantities which have been measured. A second question concerns the possibility of adverse effects on the motion pattern at the downstream end of the channel resulting from vorticity created at the entrance and carried through the conduit. These questions can be answered by experimental studies in which both channel length and entrance conditions are systematically varied.

A third question left unanswered is one concerning the mechanisms by which the secondary motions are maintained. A study of the distribution of energy over a section normal to the flow in a long, straight, non-circular channel could be expected to yield information pertinent to this problem.

APPENDIX

NUMERICAL EVALUATION OF EQUATION (13)

To test the state of development of flow at the downstream end of the channel, Equation (13) has been approximated by a difference equation to permit the substitution of experimental data into it, with the assumption that the state of development would be reflected by the degree to which the equation is satisfied. Equation (13), in expanded form, is:

$$W\frac{\partial^2 W}{\partial y \partial z} - W\frac{\partial^2 V}{\partial z^2} + V\frac{\partial^2 W}{\partial y^2} - V\frac{\partial^2 V}{\partial y \partial z} = \frac{\partial^2 \overline{vw}}{\partial z^2} - \frac{\partial^2 \overline{vw}}{\partial y^2} + \frac{\partial^2}{\partial y \partial z}\left(\overline{v^2} - \overline{w^2}\right)$$

The differential terms of the equation are of two types; the first involving the second derivative with respect to y or z, the second the cross derivative with respect to both y and z. With reference to the grid system shown below, with m designating the value of V, W, vw, or $(\overline{v^2} - \overline{w^2})$, terms of type 1 are expressible by:

$$\frac{\partial^2 m(y,z)}{\partial z^2} \approx \frac{m(y,z+\Delta z) + m(y,z-\Delta z) - 2m(y,z)}{\Delta m^2}$$

and

$$\frac{\partial^2 m(y,z)}{\partial y^2} \approx \frac{m(z,y+\Delta y) + m(z,y-\Delta y) - 2m(y,z)}{\Delta y^2}$$

	$m(y + \Delta y, z - \Delta z)$	$m(y + \Delta y, z)$	$m(y + \Delta y, z + \Delta z)$
	$m(y, z - \Delta z)$	$m(y, z)$	$m(y, z + \Delta z)$
	$m(y - \Delta y, z - \Delta z)$	$m(y - \Delta y, z)$	$m(y - \Delta y, z + \Delta z)$

Terms of the second type are evaluated from:

$$\frac{\partial^2 m(y,z)}{\partial y \partial z} \approx \frac{1}{4\,\Delta y \Delta z}\Big[m(y + \Delta y, z + \Delta z) - m(y + \Delta y, z - \Delta z)$$

$$- m(y - \Delta y, z + \Delta z) + m(y - \Delta y, z - \Delta z)\Big]$$

By expanding $m(y, z + \Delta z)$ and $m(y, z - \Delta z)$ in Taylor series, and adding, the error in the evaluation of $\frac{\partial^2 m(y,z)}{\partial z^2}$ from the approximate expression given above can be shown to be:

$$\text{Error} = -\frac{1}{12}\frac{\partial^4 m(y,z)}{\partial z^4}\Delta z^2 - \frac{1}{360}\frac{\partial^6 m(y,z)}{\partial z^6}\Delta z^4 - \ldots$$

A similar expression for $\frac{\partial^2 m}{\partial y^2}$ involves the substitution of Δy for Δz.

The error in terms of the second type can be evaluated from Taylor expansions of $m(y + \Delta y, z + \Delta z)$, $m(y + \Delta y, z - \Delta z)$, $m(y - \Delta y, z - \Delta z)$ and $m(y - \Delta y, z - \Delta z)$. From these:

$$\text{Error} \doteq \frac{1}{6}\frac{\partial^4 m(y,z)}{\partial y^3 z}(\Delta y)^2 + \frac{1}{6}\frac{\partial^4 m(y,z)}{\partial y \partial z^3}(\Delta z)^2 + \ldots.$$

While more sophisticated expressions for the derivatives could be used, it is doubtful that the added refinement is justified by the accuracy to which the variables have been measured. From inspection, the error in the evaluation of each type of derivative is of the same order of magnitude.

The component terms in the finite difference counterpart of Equation (13) have been evaluated at five points in the test section of the channel, using smoothed data. These are:

1. At the vertical centerline, at the point where V = W.
2. At the center of the lower secondary motion cell, where V = W.
3. At a point above the center of the lower vortex, where V ≈ W.
4. Near the floor, where W is large.
5. Near the sidewall, where V is large.

Perhaps not surprisingly, each of the terms at each of the selected points proved to be smaller and of a different order of magnitude than the integral values of the variables which are involved. In each case, at each point, the difference equation was satisfied; this circumstance is not convincing evidence that the motion pattern was completely developed, however, because a precise evaluation of the equation would require experimental data which is accurate beyond the capabilities of the equipment used during this study. No conclusions relative to this point have therefore been drawn.

LITERATURE CITED

1. Nikuradse, J., "Untersuchungen Über turbulente Strömungen in nicht kreisförmigen Rohren," Ingenieur-Archiv, Vol. 1, 1930, pp. 306-332.

2. Schlichting, H., "Berechnung ebener periodischer Grenzschichtströmungen," Physilkalische Zeitschrift, Vol. 33, 1932, p. 327.

3. Muller, Max, "Studien Über die Bewegung des Wassers in Flüssen mit Bezugnahme auf die Ausbildung des Flussprofiles," Zeitschrift für Bauwesen, 1883, p. 201.

4. Stearns, F. P., "On the Current Meter, Together with a Reason Why the Maximum Velocity of Water Flowing in Open Channels is Below the Surface," Transactions, American Society of Civil Engineers, Vol. 12, 1883, pp. 331-338.

5. Gibson, A. H., "On the Depression of the Filament of Maximum Velocity in a Stream Flowing Through an Open Channel," Proceedings, Royal Society of London, Series A, Vol. 82, 1909, pp. 149-159.

6. Prandtl, L., "Über die ausgebildete Turbulenz," Proceedings, 2nd International Congress for Applied Mechanics, Zurich, 1927, p. 62.

7. Casey, Hugh, "Über Geschiebebewegung," Mitteilung der Preussischen Versuchsanstalt für Wasserbau und Schiffbau, Vol. 19, 1935, Fig. 8.

8. Vanoni, Vito A., "Transportation of Suspended Sediment by Water," Transactions, American Society of Civil Engineers, Vol. 111, 1946, pp. 67-102.

9. Tracy, H. J., and C. M. Lester, "Resistance Coefficients and Velocity Distribution - Smooth Rectangular Channel," Water-Supply Paper 1592-A, U. S. Department of the Interior, Geological Survey, 1961, p. 14.

10. Bazin, H., "Recherches hydrauliques," Memoires presentes par divers savants, Science mathematiques et physiques, Series 2, Vol. 19, 1865.

11. Koloseus, H. J., "The Effect of Free-Surface Instability on Channel Resistance," Unpublished Ph.D. Thesis, State University of Iowa, 1958.

12. Nemenyi, Paul F., Discussion of "Transportation of Suspended Sediment by Water," by Vito A. Vanoni, Transactions, American Society of Civil Engineers, Vol. 111, 1946, p. 122.

13. Kirschmer, Otto, "Pertes de charge dans les conduits forcees et les canaux decouverts," Revue generale de l'hydraulique, Paris, Vol. 15, No. 51, May-June 1949, pp. 115-138.

14. Eckert, E. G. R., and T. F. Irvine, "Flows in Corners of Passages with Non-Circular Sections," Transactions, American Society of Mechanical Engineers, Vol. 78, 1956, pp. 709-718.

15. Einstein, H. A., and H. Li, "Secondary Currents in Straight Channels," Transactions, American Geophysical Union, Vol. 39, December 1958, pp. 1085-1088.

16. Gessner, F. B., and J. B. Jones, "A Preliminary Study of Turbulence Characteristics of Flow Along a Corner," Journal of Basic Engineering, American Society of Mechanical Engineers, December 1961.

17. Delleur, J. W., and D. S. McManus, "Secondary Flow in Straight Open Channels," Proceedings, Sixth Midwestern Conference on Fluid Mechanics, University of Texas, September 1959.

18. Kennedy, R. J., and J. F. Fulton, "The Effect of Secondary Currents Upon the Capacity of a Straight Open Channel," Transactions, Engineering Institute of Canada, Vol. 5, No. 1, 1961, pp. 12-18.

19. Ducoff, Arnold L., "A Report on the Design, Construction, Operation, and Preliminary Calibrations on the Low-Turbulence Wind Tunnel at the Georgia Institute of Technology," Unpublished Report, Navy Department, ONR, Contract No. Nonr. -991(01), May 1956.

20. Schubauer, G. D., and P. S. Klebanoff, "Theory and Application of Hot-Wire Instruments in the Investigation of Turbulent Boundary Layers," Report W-86, National Advisory Committee for Aeronautics, 1946.

21. Hinze, J. O., Turbulence, New York: McGraw-Hill Book Company, Inc., 1959, pp. 81-102.

22. Laufer, John, "Investigation of Turbulent Flow in a Two-Dimensional Channel," Report 1053, National Advisory Committee for Aeronautics, 1951.

23. MacMillan, F. A., "Experiments on Pitot-Tubes in Shear Flow," Aeronautical Research Council (Brit.), Reports and Memoranda No. 3028, February 1956.

24. Reichart, H., "Messungen turbulenter Schwankungen," Die Naturwissenschaften, Jahrig 26, Heft 24-25, June 1938, pp. 404-408.

25. Laufer, John, "The Structure of Turbulence in Fully Developed Pipe Flow," National Advisory Committee for Aeronautics, Report 1174, 1954.

26. Fage, A., and H. C. H. Townend, "An Examination of Turbulent Flow with an Ultramicroscope," Proceedings of the Royal Society (London), Series A, Vol. 135, No. 828, April 1, 1932, pp. 656-677.

VITA

Hubert J. Tracy was born in Little Rock, Arkansas on February 18, 1918. He received his elementary and secondary education in the public schools of that city, and graduated from Little Rock High School in June, 1935. He received a BSCE degree from the University of Arkansas in June, 1939.

After a number of jobs of a temporary nature, he accepted employment as a hydraulic engineer with the U. S. Geological Survey in Fort Smith, Arkansas in August, 1940. He was called into active military service in June, 1941 with the Corps of Engineers, U. S. Army. He was sent to the China-Burma-India theater in April, 1944 as a Company Commander with the 1880th Engineer Battalion, and participated in the construction of the Ledo Road in northern India, and north and central Burma. He returned to the United States in early 1946 and was discharged with the rank of Captain.

After his discharge, he returned to the U. S. Geological Survey, and was assigned to the Baton Rouge, Louisiana office. He was transferred to Lincoln, Nebraska in 1948, where he remained until 1950, when he took leave of absence to obtain a Master of Science degree from Louisiana State University. After the year of graduate study, he returned to the U. S. Geological Survey in Topeka, Kansas, and was shortly thereafter transferred to Atlanta, Georgia.

In Atlanta, where he has remained until the present time, he was assigned to research work in the field of open-channel flow, which was

conducted at the Georgia Institute of Technology under a cooperative agreement between the Institute and the U. S. Geological Survey. In 1956, he entered the Graduate Division at the Institute and began work on the Ph.D. degree on a part-time basis.

He is the author of numerous research reports on open-channel flow. He is unmarried, and is a member of the American Society of Civil Engineers, the American Geophysical Union, and the International Association for Hydraulic Research.